Issues in Palatini $\mathcal{R}^2$ inflation: Bounds on the reheating temperature

A. B. Lahanas*

Department of Physics, Nuclear and Particle Physics Section,
National and Kapodistrian University of Athens, GR–157 71 Athens, Greece

(Received 31 October 2022; accepted 14 December 2022; published 30 December 2022)

We consider $\mathcal{R}^2$ inflation in Palatini gravity, in the presence of scalar fields coupled to gravity. These theories, in the Einstein frame, and for one scalar field h, share common features with K-inflation models. We apply this formalism for the study of single-field inflationary models, whose potentials are monomials, $V \sim h^n$, with n a positive even integer. We also study the Higgs model nonminimally coupled to gravity. With $\mathcal{R}^2$ terms coupled to gravity as $\sim\alpha\mathcal{R}^2$, with α constant, the instantaneous reheating temperature T_{ins}, is bounded by $T_{ins} \leq 0.290 m_{\text{Planck}}/\alpha^{1/4}$, with the upper bound being saturated for large α. For such large α need go beyond slow roll to calculate reliably the cosmological parameters, among these the end of inflation through which T_{ins} is determined. In fact, as the inflaton rolls towards the end of the inflation point, the quartic in the velocity terms, unavoidable in Palatini gravity, play a significant role and cannot be ignored. The values of α, and other parameters, are constrained by cosmological data, setting bounds on the inflationary scale $M_s \sim 1/\sqrt{\alpha}$ and the reheating temperature of the Universe.

DOI: 10.1103/PhysRevD.106.123530

I. INTRODUCTION

The Palatini formulation of general relativity (GR), or first-order formalism, is an alternative to the well-known metric formulation, or second-order formalism. In the latter the space time connection is determined by the metric while in the Palatini approach the connection $\Gamma^{\mu}_{\lambda\sigma}$ is treated as an independent variable [1–9]. It is through the equations of motion that $\Gamma^{\mu}_{\lambda\sigma}$ receive the well-known form of the Christoffel symbols, describing thus a metric connection. Within the context of GR the two formulations are equivalent. However in the presence of fields that are coupled in a nonminimal manner to gravity this no longer holds [1–3], and the two formulations describe different physical theories.

Encompassing the popular inflation models into Palatini gravity, in an effort to describe the cosmological evolution of the Universe, leads to different cosmological predictions, from the metric formulation, due to the fact that the dynamics of the two approaches differ. A notable example is the Starobinsky model, for instance, where except the graviton there exists an additional propagating scalar degree of freedom, the scalaron, whose mass is related to the coupling of the $\mathcal{R}^2$ term. In the Einstein frame this emerges as a dynamical scalar field, the inflaton, moving under the influence of the celebrated Starobinsky potential [10–12]. Within the framework of the Palatini gravity, in any $f(\mathcal{R})$ theory [3], there are no extra propagating degrees of freedom that can play the role of the inflaton, and hence the inflaton has to be put in by hand as an additional scalar degree of freedom.

The differences between metric and Palatini formulation in the cosmological predictions, as far as inflation is concerned, arise from the nonminimal couplings of the scalars, that take up the role of the inflaton. These couplings are different in the two approaches. This has been first pointed out in [13] and has attracted the interest of many authors since Refs. [14–52], with still continuing activity [53–83].

Measurements of the cosmological parameters, by various collaborations, has tighten the allowed window of these observables which in turn constrain, or even exclude, particular inflationary models [84–87]. In particular, the spectral index n_s and the bounds on the tensor-to-scalar ratio r impose severe restrictions and not all models can be compatible with the observational data.[1] The precise measurements of the primordial scalar perturbations, and of the associated power spectrum amplitude A_s, imply constraints for the scale of inflation in models encompassed in the framework of the metric or Palatini formulation, which are more stringent in the case of Palatini gravity as has been shown in [51].

In this work we shall consider $\mathcal{R}^2$ theories, in the framework of the Palatini gravity, and study the cosmological predictions of some popular models existing in literature, with emphasis on the maximal reheating

*alahanas@phys.uoa.gr

[1]In this work, standard assumptions are made for neutrino masses and their effective number. Relaxing these it induces substantial shifts in n_s [88].

temperature, or instantaneous reheating temperature. We will show that there are strict theoretical bounds on it which are saturated when the couplings α, associated with the $\mathcal{R}^2$ term, are large. To this goal we need go beyond the slow-roll approximation, to extract reliable predictions, since quartic in the velocity terms of the inflaton play a crucial role. Assuming instantaneous reheating, the cosmological data impose upper bounds on α, or similarly, lower bounds on the inflationary scale, which also hold for lower reheating temperatures.

This paper is organized as follows:

In Sec. II, we present the salient features and give the general setup of $f(\mathcal{R})$-Palatini gravity,[2] in the presence of an arbitrary number of scalar fields, coupled to Palatini gravity in a nonminimal manner, in general. Although this is not new, as this effort has been undertaken by other authors, as well, we think that the general, and model-independent, expressions we arrive at, are worth being discussed. We focus on $\mathcal{R}^2$ theories for which the passage to the Einstein frame is analytically implemented. These theories have a gravity sector, specified by two arbitrary functions, sourcing, in general, nonminimal couplings of the scalars involved in Palatini gravity, and a third function which is the scalar potential. In the Einstein frame, and when a single field is present, these models have much in common with the K-inflation models [89].

In Sec. III, we discuss the arising background equations of motions and discuss the slow-roll mechanism, paying special attention to the end of inflation and its validity within the slow-roll scheme. We find that in some cases we need to go beyond slow-roll to determine the end of inflation, which controls the instantaneous reheating temperature and the cosmological parameters.

In Sec. IV we discuss various aspects of the inflationary evolution of these models, in the general case, and extract useful conclusions, which hold even when the evolution of inflaton, as it approaches the minimum of the scalar potential, deviates significantly from slow-roll.

Section V deals with the instantaneous reheating temperature and its bounds set on it, which are dictated by the pertinent background equations. Strict upper bounds are derived which are saturated when the parameter α, defining the coupling of the $\mathcal{R}^2$ terms to gravity, is large. These could not have been predicted within the slow-roll scheme. Moreover, assuming that reheating is instantaneous, we explore the bounds set by the cosmological observables, on the parameters of particular inflation models; namely, the class of models in which the scalar field h is characterized by monomial potentials $\sim h^n$, with n a positive even integer, and the Higgs model. The power spectrum amplitude A_s results to fine-tuning of the parameters of the potential, while the spectral index n_s and the tensor to scalar ratio r, set bounds on α, and therefore bounds on the inflation scale and the instantaneous reheating temperature, $T_{\rm ins}$. The latter can be as large as $\sim 10^{15}$ GeV, the larger values attained for the smaller allowed value of the parameter α.

In Sec. VI, we end up with our conclusions.

[2]Throughout this paper the Ricci scalar will be denoted by $\mathcal{R}$.

II. THE MODEL

In this section we outline the general setup, and follow the methodology and notation used in [51]; more details, if needed, can be found in this reference. The starting point is an action involving scalar fields h^J which are coupled to Palatini gravity in the following manner,

$$S=\int d^4x\sqrt{-g}\left(f(\mathcal{R},h)+\frac{1}{2}G_{IJ}(h)\partial h^I\partial h^J-V(h)\right). \quad (1)$$

In it $\mathcal{R}$ is the scalar curvature, in the Palatini formalism, and $f(\mathcal{R},h)$ an arbitrary function of the scalars h^J and $\mathcal{R}$. Following standard procedure we write this action in the following manner, introducing an auxiliary field Φ,

$$S=\int d^4x\sqrt{-g}\left(f(\Phi,h)+f'(\Phi,h)(\mathcal{R}-\Phi)+\frac{1}{2}G_{IJ}(h)\partial h^I\partial h^J-V(h)\right). \quad (2)$$

In this $f'(\Phi,h)$ denotes the derivative with respect Φ. This action can be written as follows, in Jordan frame,

$$S=\int d^4x\sqrt{-g}\left(\psi\mathcal{R}+\frac{1}{2}G_{IJ}(h)\partial h^I\partial h^J-\psi\Phi+f(\Phi,h)-V(h)\right), \quad (3)$$

where ψ in defined by

$$\psi=\frac{\partial f(\Phi,h)}{\partial\Phi},\ \text{with inverse}\ \Phi=\Phi(\psi,h). \quad (4)$$

One can go to the Einstein frame by performing a Weyl transformation of the metric

$$g_{\mu\nu}=\bar{g}_{\mu\nu}/2\psi \quad (5)$$

and that done the theory receives the following form,

$$S=\int d^4x\sqrt{-\bar{g}}\left(\frac{\bar{\mathcal{R}}}{2}+\frac{1}{4\psi}G_{IJ}(h)\partial h^I\partial h^J-\frac{1}{4\psi^2}(\psi\Phi-f(\Phi,h)+V(h))\right). \quad (6)$$

We can further eliminate the field ψ, using its equation of motion,

$$\psi(\partial h)^2 = \psi\Phi - 2f(\Phi, h) + 2V(h), \tag{7}$$

where, in order to speed up notation, we have denoted $G_{IJ}(h)\partial h^I \partial h^J = (\partial h)^2$. Note that (7) is not solvable, in general, however in $\mathcal{R}^2$ theories this is feasible.

In the following we shall focus on such theories, with a single field h present, with $f(h, \mathcal{R})$ quadratic in the curvature, having therefore the form

$$f(\mathcal{R}, h) = \frac{g(h)}{2}\mathcal{R} + \frac{\mathcal{R}^2}{12M^2(h)}. \tag{8}$$

Since a single scalar field is assumed its kinetic term can be always brought to the form $(\partial h)^2/2$, that is in the action (1) the field can be taken canonically normalized. Therefore in this theory there are three arbitrary functions, namely, $g(h), M^2(h), V(h)$, and any choice of them specifies a particular model. We have set the reduced Planck mass $m_{\rm Planck} \equiv m_P = (8\pi G_N)^{-1/2}$ dimensionless and equal to unity and thus all quantities in (8) are dimensionless. When we reinstate dimensions the functions g, V have dimensions mass^2, mass^4, respectively, while M^2 is dimensionless. Note that a nontrivial field dependence of the functions $g(h)$, and/or $M^2(h)$, is a manifestation of nonminimal coupling of the scalar h to Palatini gravity. We recall that in Palatini formalism there is not a scalaron field, associated with an additional propagating degree of freedom, which in the Einstein frame of the metric formulation plays the role of the inflaton.

With the function $f(\mathcal{R}, h)$, as given by (8), we get from Eq. (4),

$$\psi = \frac{g(h)}{2} + \frac{\Phi}{6M^2(h)}, \tag{9}$$

and (7) is solved for ψ in a trivial manner, yielding

$$\psi = \frac{4V + 3M^2 g^2}{2(\partial h)^2 + 6M^2 g}. \tag{10}$$

In this way ψ, and hence Φ, from (9), are expressed in terms of $h, (\partial h)^2$. Plugging ψ, Φ into (6) we get, in a straightforward manner

$$S = \int d^4x\sqrt{-g}\left(\frac{\mathcal{R}}{2} + \frac{K(h)}{2}(\partial h)^2 + \frac{L(h)}{4}(\partial h)^4 - U_{\rm eff}(h)\right). \tag{11}$$

In this action we have suppressed the bar in the scalar curvature and also in $\sqrt{-g}$, and in order to simplify notation we have denoted $\partial_\mu h \partial^\mu h$ by $(\partial h)^2$ and $(\partial_\mu h \partial^\mu h)^2$ by $(\partial h)^4$. Note the appearance of quartic terms $(\partial h)^4$ in the action. As for the functions $K, L, U_{\rm eff}$, appearing in (11), they are analytically given by

$$L(h) = (3M^2 g^2 + 4V)^{-1}, \qquad K(h) = 3M^2 gL,$$
$$U_{\rm eff} = 3M^2 VL. \tag{12}$$

Observe that since terms up to $\mathcal{R}^2$ have been considered, in $f(\mathcal{R}, h)$, higher than $(\partial h)^4$ terms do not appear in the action (11).

The above Lagrangian may feature, under conditions, K-inflation models [89], which involve a single field, described by an action whose general form is

$$S = \int \sqrt{-g}\left(\frac{\mathcal{R}}{2} + p(h, X)\right)d^4x, \tag{13}$$

where $X \equiv (1/2)\partial_\mu h \partial^\mu h$. The cosmological perturbations of such models were considered in [90] and the importance of a time-dependent speed of sound c_s in K-inflation models was emphasized in [91] and cosmological constraints were derived, where improved expressions for the density perturbations power spectra were used. Specific models were also considered in [92]. See also Refs. [93–98], for more recent works on these models, in various contexts.

In a flat Robertson-Walker metric, where the background field h is only time dependent, the energy density and pressure are given by

$$\rho(h, X) = K(h)X + 3L(h)X^2 + U_{\rm eff}(h),$$
$$p(h, X) = K(h)X + L(h)X^2 - U_{\rm eff}(h), \tag{14}$$

with X being, in this case, half of the velocity squared, $X = \dot{h}^2/2$.

We shall assume that the function $L(h)$ is always positive to avoid phantoms, which may lead to an equation of state with $w < -1$. This may occur when $L < 0$ and X becomes sufficiently large. However, there is no restriction on the sign of $K(h)$ which may be negative in some regions of the field space, signaling that the kinetic term has the wrong sign in those regions. Obviously the sign of $K(h)$ should be positive at the minimum of the potential. Options where K is negative in some regions, although interesting, will not be pursued in this work. Besides, we shall assume that the potential is positive $U_{\rm eff}(h) \geq 0$ and bears a Minkowski vacuum. This ensures that the energy density is positive definite even when the velocity is vanishing. The location of the Minkowski vacuum can be taken to be at $h = 0$, without loss of generality, by merely shifting appropriately the field h. Then having a positive definite potential which vanishes at $h = 0$ entails $U_{\rm eff}(0) = 0$ and also $U'_{\rm eff}(0) = 0$. When inflation models are considered, the inflaton will roll down towards this minimum signaling the end of inflation and beginning of Universe thermalization.

Concerning the potential $U_{\rm eff}$, appearing in the Lagrangian (11) in the Einstein frame, using Eq. (12) it is trivially shown that it can be cast in the following form,[3]

$$U_{\rm eff}=\frac{1}{4}\left(3M^2-\frac{1}{R}\right)=\frac{3M^2}{4}(1-gK)\quad \text{where } R=\frac{L}{K^2}. \tag{15}$$

The two forms of the potential above are equivalent, if the relation $K=3M^2gL$ of Eq. (12) is used. The quantity R appearing in this equation may play an important role, as we shall see, in inflationary evolution. From Eq. (15) we see that positivity of $U_{\rm eff}\geq 0$ entails to having $R^{-1}\leq 3M^2$. In terms of the potential $V(h)$ appearing in the action (1) this simply reads $V\geq 0$, as can be seen from the last of Eqs. (12). Dealing with positive definite potentials, an upper bound is then established,

$$U_{\rm eff}\leq\frac{3M^2}{4}, \tag{16}$$

as is evident from (15). Although not necessary, this upper bound can be easily saturated, for large h, by choosing appropriately the functions involved. Actually the asymptotic behavior of these functions, for large h, control the behavior of the potential in this regime. Choosing, for instance, the function R to increase, as h becomes large, then saturation of the above bound is easily obtained. If, moreover, we opt that the function M^2 approaches or even be a constant, for large h values, while the function R increases in this regime, then the potential reaches a plateau which may yield enough inflation. This is a rather plausible scenario, which may drive successful inflation, and is obtainable under rather mild assumptions. However, other less obvious choices may be available.

The models studied in this work can be, in general, classified in three main categories:

(i) Models with $g, M^2=$ constants, named **M1** for short for future reference.

These are dubbed minimally coupled models. In this case the constant g can be taken equal to unity without loss of generality. This is implemented by rescaling the metric as $g_{\mu\nu}\to g_0^{-1}g_{\mu\nu}$, where $g_0=g$, accompanied by a redefinition of the field $h\to g_0^{1/2}h$ in the action (1), with $f(\mathcal{R},h)$ as given by (8), before going to Einstein frame.

(ii) Models with $M^2=$ constant and g a function of h. These we name **M2** for short.

In this class of models g can be a function of the field h, $g(h)$. In this case we can take $g(0)=1$ by rescaling the metric and the field h, in the way described previously for the M1 models, with g_0 identified with $g(0)$. In both cases, M1 or M2, it is tacitly assumed that $g_0>0$.

(iii) Models with both g, M^2 functions of h. These we shall name **M3**.

The models $M1, M2$ cover a broad range of interesting models, studied in the past in various contexts, and shall concern us most. Models belonging to the class M_3 have been studied in [61].

As discussed, we shall be interested in models with positive semidefinite potential having a single Minkowski vacuum at a point, which without loss of generality we can take it to be located at $h=0$. Then, besides $U_{\rm eff}>0$, we must have $\frac{dU_{\rm eff}}{dh}>0$ for $h>0$, with the sign of the derivative reversed when $h<0$. These imply restrictions for the functions describing the aforementioned models. For instance, for the minimally coupled models this entails $\frac{dK}{dh}<0(>0)$ for $h>0(h<0)$, using Eq. (15) and the fact that $g>0$. The above requirements are rather mild and can be easily satisfied. Therefore many options are available for scalar potentials bearing the characteristics demanded for successful inflation to be possibly implemented. This will be exemplified in specific models, to be discussed later.

Concluding this section, we presented a general, and model independent, framework of $\mathcal{R}^2$ theories, in the Palatini formulation of gravity, which may be useful for the study of inflation. In the Einstein frame these theories may be considered as generalizations of K-inflation models. This formalism will be implemented, for the study of particular inflationary models.

III. THE EQUATIONS OF MOTION AND THE SLOW-ROLL

A. The inflationary equations of motion

When noncanonical kinetic terms are present the equations of motion for the would-be inflaton scalar field h differ from their standard form. As a result, the cosmological parameters describing the slow-roll evolution should be modified appropriately. Certainly one can normalize the kinetic term of the scalar field appropriately but this is not always very convenient. Actually the integrations needed, in order to pass from the noncanonical to a canonically normalized field, in most of the cases, cannot be carried out analytically. Therefore it proves easier, in certain cases, to work directly with the noncanonical fields and express the pertinent cosmological observables in a manner that is appropriate for this treatment.

It is not hard to see that the field h satisfies the equation of motion given by

$$(K+3L\dot{h}^2)\ddot{h}+3H(K+L\dot{h}^2)\dot{h}+U'_{\rm eff}(h)+\frac{1}{4}(2K'+3L'\dot{h}^2)\dot{h}^2=0, \tag{17}$$

[3]The quantity R should not be confused with the Ricci scalar $\mathcal{R}$.

where dots denote derivatives with respect to time. If the field were canonical, $K = 1$, and there were no quartic in the velocity terms, that is $L = 0$, the equation above receives a much simpler form. In this, the effect of using a noncanonical, in general, field h is encoded in the function K. The effect of the presence of terms $(\partial h)^4$ in the action is encoded within the function L. The terms that depend on L are multiplied by an extra power of the velocity squared, as compared to the K terms. These cannot be neglected, as we discuss below, since they are not small in general.

We can gain more insight if we use a canonically normalized field, say ϕ, defined by

$$\phi = \int_0^h \sqrt{K(h)}dh, \tag{18}$$

which, however, cannot be always presented in a closed form, as we have already remarked. The constant of integration has been chosen, without loss of generality, so that $h = 0$ corresponds to the value $\phi = 0$ too. To avoid ghosts we shall assume that $K > 0$, so that the integration above makes sense. Actually if K is negative the kinetic term of the field ϕ would have the wrong sign, i.e., it would appear as $-(\partial\phi)^2$. It could happen however that this function is negative in some region but at the Minkowski vacuum is strictly positive. In this way ghosts are also avoided. This case, interesting as might be, is not discussed and we prefer to keep a rather conservative view point and take $K > 0$ in the whole region. Then in terms of the field ϕ the equation of motion (17) takes on the form

$$(1 + 3R\dot{\phi}^2)\ddot{\phi} + 3H(1 + R\dot{\phi}^2)\dot{\phi} + \frac{dU_{\rm eff}}{d\phi} + \frac{3}{4}\frac{dR}{d\phi}\dot{\phi}^4 = 0. \tag{19}$$

Note the dependence of this equation on the ratio $R = L/K^2$ defined earlier in Eq. (15). From this form it appears that the smallness of the ∂h^4 terms in the action is quantified by the smallness of the ratio $\frac{L}{K^2}\dot{\phi}^2 \ll 1$, which is equivalent to $\frac{L}{K}\dot{h}^2 \ll 1$.

The equation governing the evolution as functions of time can be easily converted to differential equation for the velocities as function of the fields. This is done by noting that there is no explicit dependence on time in either of (17) or (19). The velocity of h field, $u(h)$ satisfies

$$(K + 3Lu^2)u\frac{du}{dh} + 3H(K + Lu^2)u + U'_{\rm eff}(h) + \frac{1}{4}(2K' + 3L'u^2)u^2 = 0, \tag{20}$$

which is a first order equation with respect the velocity $u(h)$. The velocity $\dot{h}$ and the acceleration $\ddot{h}$, as functions of h, in Eq. (20) are given by

$$\dot{h} = u(h), \qquad \ddot{h} = u(h)\frac{du(h)}{dh}. \tag{21}$$

This method is well known in mathematics.[4]

By the same token, for the normalized inflaton field ϕ, we have

$$(1 + 3Rv^2)v\frac{dv}{d\phi} + 3H(1 + Rv^2)v + \frac{dU_{\rm eff}}{d\phi} + \frac{3}{4}\frac{dR}{d\phi}v^4 = 0, \tag{22}$$

where, in this case, the velocity $\dot{\phi}$ and the acceleration $\ddot{\phi}$, as functions of ϕ, are given by

$$\dot{\phi} = v(\phi), \qquad \ddot{\phi} = v(\phi)\frac{dv(\phi)}{d\phi}. \tag{23}$$

Equations (20) and (22), being first order equations, are more easily solved for values of the fields lying in the inflationary regime.

B. Is slow-roll a valid scenario?

The usual slow-roll solution is not a valid approximate solution for any values of the parameters involved. This can be exemplified in certain models, as we shall see. To be more specific, in the class of models where $M^2 =$ constant, which we study in this work, Eq. (19) takes on the form, using Eq. (15),

$$(1 + 3R\dot{\phi}^2)\ddot{\phi} + 3H(1 + R\dot{\phi}^2)\dot{\phi} + (1 + 3R^2\dot{\phi}^4)\frac{dU_{\rm eff}}{d\phi} = 0. \tag{24}$$

where the Hubble function is given by

$$3H^2 = \left(1 + \frac{3}{2}R\dot{\phi}^2\right)\frac{\dot{\phi}^2}{2} + U_{\rm eff}. \tag{25}$$

Neglecting $R\dot{\phi}^2$ in the equations above we recover the well-known form of the Friedmann equation for the canonically normalized field ϕ. In the regime $R\dot{\phi}^2 \ll 1$ slow-roll evolution is realized. Using the slow-roll expressions one can see, in a straightforward manner, that

$$R\dot{\phi}^2 = \frac{2RU_{\rm eff}}{3}\epsilon_V(\phi), \tag{26}$$

[4]The points at which u vanishes correspond to "cusp" points. There the acceleration $\frac{du}{dh}$ becomes infinite. There are no cusp points from the beginning of inflation up to values of the field for which u vanishes for first time. This covers the whole inflation region.

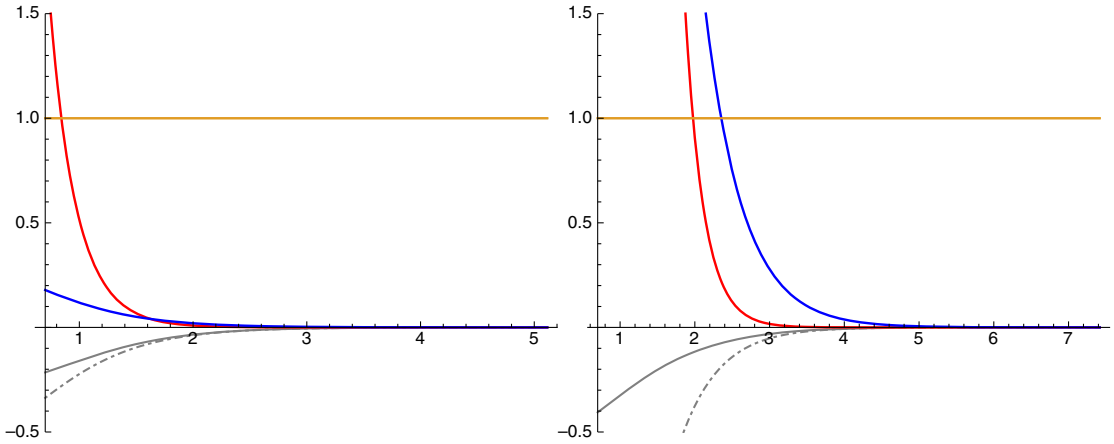

FIG. 1. Evolution of ϵ_V, red line, and $R\dot{\phi}^2$, blue line, in the slow-roll approximation in Model I as functions of $\sqrt{c}\phi$. On the left, $c = 0.845$ corresponding to $\alpha = 10^{10}$ and on the right $c = 0.845 \times 10^2$ corresponding to $\alpha = 10^{12}$. In both cases the parameter m is $m = 6.5 \times 10^{-6}$.

which holds provided $R\dot{\phi}^2$ is small enough. In this equation $\epsilon_V = \frac{1}{2}(U'_{\rm eff}(\phi)/U_{\rm eff}(\phi))^2$. However the smallness of $\epsilon_V(\phi)$ does not ensure smallness of $R\dot{\phi}^2$. This is shown in Fig. 1 for the minimally coupled model, described by the potential $V = m^2h^2/2$ and $g = 1$, $M^2 = 1/3\alpha$. In this class of models both ϵ_V and $R\dot{\phi}^2$ depend only on the combination $c = 2\alpha m^2$. We have fixed m by taking it to be $m = 6.5 \times 10^{-6}$, or so, suggested by primordial scalar perturbations, as we shall see later. The horizontal axis is $\sqrt{c}\phi$. For the case shown on the left, $c = 0.845$, corresponding to $\alpha = 10^{10}$, while on the right $c = 0.845 \times 10^2$, corresponding to $\alpha = 10^{12}$. Notice the difference in the behavior of the $\epsilon_V(\phi)$ (red solid line) and $R\dot{\phi}^2$ (blue solid line) functions. For the lower c case, $R\dot{\phi}^2$ stays lower than unity all the way up to the point where $\epsilon_V = 1$, marked by the yellow horizontal line. In this case the usual slow-roll scenario is trusted. The gray line is the exact solution for the velocity $v(\phi)$, scaled by $1/\sqrt{a}$, that is $v(\phi)/\sqrt{a}$, which has been derived numerically. The gray dot-dashed line is the corresponding slow-roll approximation. These start deviating significantly, from each other, as soon as $R\dot{\phi}^2$ starts becoming sizable. Note that for the larger c-case displayed, this occurs well before $\epsilon_V(\phi)$ becomes unity, showing that slow-roll ceases to be a good approximation although $\epsilon_V(\phi)$ is significantly lower than unity. The conclusion is that, for lower c, corresponding to lower α, $R\dot{\phi}^2$ is small, and the slow-roll solution is a good approximation. On the contrary, for large c values, $R\dot{\phi}^2$ becomes large before $\epsilon_V = 1$. Therefore slow-roll in the usual sense can be only realized in the region of ϕ values for which $R\dot{\phi}^2$ is small, and thus far from the point where $\epsilon_V = 1$. The evaluation of the end of inflation, in this case, can be only achieved numerically since approximate slow-roll solutions, based on $\epsilon_V = 1$, cannot be trusted in the region of ϕ for which $R\dot{\phi}^2$ starts approaching unity.

Concerning the end of inflation, this takes place when the parameter $\epsilon_1 = -\dot{H}/H^2$ becomes equal to unity. In the slow-roll regime, where $R\dot{\phi}^2$ are negligible, ϵ_V and ϵ_1 almost coincide, assuming de Sitter expansion, but this is not the case when $R\dot{\phi}^2$ terms start growing and the approximate slow-roll solution no longer holds. Therefore we rely on $\epsilon_1 = 1$ as the only reliable means to determine accurately the end of inflation. This is equivalent to $\rho + 3p = 0$, corresponding to $\ddot{a} = 0$ for the cosmic scale factor, and yields the following relation between the velocity and field value, at time ϵ_1 reaches unity,

$$v^2(\phi) = \frac{2}{3R}(-1 + \sqrt{1 + 3RU_{\rm eff}}). \tag{27}$$

In this $v(\phi)$ is the velocity $\dot{\phi}$ expressed as a function of the field ϕ, and can be extracted numerically by solving (22). In ordinary inflation models where the R terms are missing, that is there are no terms quartic in the velocity in the action, the analog of Eq. (27) is $v^2(\phi) = U_{\rm eff}$, a well-known result, and this can be solved to yield the value of the field $\phi_{\rm end}$ at end of inflation, if the slow-roll solution is used. This is actually equivalent to $\epsilon_V = 1$.[5] If the R terms are sizable, before the end of inflation, we lack even an approximate solution for $v(\phi)$, and thus (27) can be only tackled numerically, in order

[5]When the inflaton kinetic energy is $\dot{\phi}^2/2$, the condition $\epsilon_1 = 1$ corresponds actually to $\epsilon_H(\phi) = 1$, where $\epsilon_H(\phi), \eta_H(\phi)$ are slow-roll parameters defined in [99]. Thus $\phi_{\rm end}$ extracted from $\epsilon_V = 1$ can be considered as a first-order result. An improved value for $\phi_{\rm end}$, using the exact relation $\epsilon_H(\phi) = 1$, can follow using $\epsilon_V = (1 + \sqrt{1 - \eta_V/2})^2$ [100]. To our knowledge, there is no such a relation when the R terms are present, which would approximate (27).

to know $\phi_{\rm end}$. In fact using the slow-roll parameter ϵ_V to determine the end of inflation overestimates the value $\phi_{\rm end}$, as this is extracted from (27), leading to erroneous results concerning cosmological observables, and in particular the energy density at the end of inflation, which determines the reheating temperature of the Universe.

It should be stressed that our numerical study duly takes into account the contribution of these terms and no approximation, whatsoever, is made. We have found numerically that they can be indeed small, [31–33,38], however this holds in a restricted range of the parameters and is not a general feature. For instance, in the nonminimal model discussed previously, with $V \sim h^2$, the combination $c = 2\alpha m^2$ has to be smaller than about unity, for these terms to be small in the entire inflationary region.

IV. INFLATIONARY EVOLUTION—END OF INFLATION

The end of inflation is signaled when $\epsilon_1 = 1$, or, equivalently, when acceleration ends, $\ddot{a} = 0$. The determination of the end of inflation requires augmented accuracy, at least in some models, as we shall discuss in the sequel. The slow-roll parameter ϵ_1 is very small during the de Sitter phase and then starts increasing; eventually becoming equal to unity where Universe acceleration stops. In order to locate when this occurs we find it useful to have an expression for the time derivative of it. ϵ_1 can be expressed in the following way:

$$\epsilon_1 = \frac{3}{2}\frac{\rho + p}{\rho} = \frac{3}{2}\frac{V^2 + RV^4}{\rho}, \tag{28}$$

where V is the velocity $V = \dot{\phi}$ and $R \equiv L/K^2$. Note that the numerator does not explicitly depend on the potential. Then the time derivative of ϵ_1 is of the form

$$\dot{\epsilon}_1 \equiv \frac{d\epsilon_1}{dt} = \frac{\mathcal{N}}{\rho^2}, \tag{29}$$

where the numerator $\mathcal{N}$ is found to be

$$\mathcal{N} = 2V\dot{V}\left(-\frac{RV^4}{4} + (1 + 2RV^2)U_{\rm eff}\right) + \left(-\frac{V^2}{4} + U_{\rm eff}\right)V^5R' - (1 + RV^2)V^3U'_{\rm eff}. \tag{30}$$

In this all primed quantities are derivatives with respect to ϕ.

We assume that the evolution starts from an initial position $h > 0$ on the plateau of the potential, or in terms of the canonically normalized inflaton field $\phi > 0$. Recall the two fields are related by $\phi = \int \sqrt{K}dh$, and we have chosen the integration constant so that $\phi = 0$ corresponds to $h = 0$ too. The potential is positive definite and exhibits a zero at $h = 0$ and as a consequence at $\phi = 0$, if expressed in terms of ϕ. Due to its positivity the first derivative of the potential vanishes at the minimum as well.

The inflaton start its journey with a very small, or even vanishing initial velocity, which soon becomes negative $V < 0$ and increases in magnitude, as inflaton rolls towards the minimum of the potential. At some time its direction is reversed. Therefore there is a time $t_{\rm acc}$ for which its acceleration vanishes, $\dot{V}(t_{\rm acc}) = 0$, while $V(t_{\rm acc}) < 0$. Then $\dot{V} > 0$ for $t > t_{\rm acc}$ and thus the velocity increases and eventually at some time t_1 it vanishes for the first time, i.e., $V(t_1) = 0$. Therefore the picture is that $V < 0$, as long as $t < t_1$, attaining its minimum value at $t_{\rm acc}$, and at the time t_1 it vanishes. At this time the acceleration is still positive, i.e., the velocity continuously being increased past the time t_1. It takes some time after it vanishes, reverses its direction, and starts oscillating about the minimum of the potential.

From the equation of motion (19) for the field ϕ, we have, therefore, that at this time t_1,

$$\left(\dot{V} + \frac{dU_{\rm eff}}{d\phi}\right)\Big|_{t_1} = 0. \tag{31}$$

However, since, as we have discussed, $\dot{V}(t_1) > 0$ it follows from the equation above that $\frac{dU_{\rm eff}}{d\phi}|_{t_1} < 0$. During the inflaton's journey, up to the time it reaches the minimum of potential, we have that $\frac{dU_{\rm eff}}{d\phi} \geq 0$, with the minimum being reached at time t_0 and for later times it becomes negative. Therefore t_0 is prior to t_1, $t_0 < t_1$. That is the minimum of the potential, which is located at $\phi = 0$, or $h = 0$, reached before the velocity vanishes for the first time during inflation, which is a rather expected behavior.

From the previous discussion we concluded that the time $t_{\rm acc}$, at which the acceleration of ϕ vanishes, and hence the velocity V takes its minimum value, is prior to t_1. Its location relative to t_0, the time the inflaton reaches the minimum of the potential, may be derived as follows. The acceleration is determined from the equations of motion. Using the fact that $U_{\rm eff}, U'_{\rm eff}$ vanish at t_0 we have that

$$\dot{V}(t_0) = -\frac{1}{1 + 3RV^2}\left(3H(1 + RV^2)V + \frac{3}{4}R'V^4\right)\Big|_{t_0}, \quad \text{where } R' = \frac{dR}{d\phi}. \tag{32}$$

Due to the fact that $V(t_0)$ is negative, we have, from this equation, that the acceleration $\dot{V}(t_0)$ is positive if $R'_0 = R'(t_0) \leq 0$. The sign of R'_0 is related to the derivative of the potential since

$$\frac{dU_{\rm eff}}{d\phi} = \frac{3}{4}\frac{dM^2}{d\phi} + \frac{1}{4R^2}\frac{dR}{d\phi}. \tag{33}$$

This conclusion can be drawn using the form of the potential as given by Eq. (15), which is valid for any M^2. From this it directly follows, using the fact that the derivative of the potential vanishes at $\phi = 0$, corresponding to t_0,

$$R_0' = -3R_0^2 M_0^{2\prime} \quad \text{where } M_0^{2\prime} = \left.\frac{dM^2}{d\phi}\right|_{\phi=0}. \tag{34}$$

Therefore $R_0' \leq 0$ in all models with $M_0^{2\prime} \geq 0$ and as a consequence $\dot{V}(t_0) > 0$. This states that t_0 lies in a region where the acceleration is positive, and this occurs after $t_{\rm acc}$. Therefore in models with $M_0^{2\prime} \geq 0$ we have that $t_{\rm acc} < t_0$. The models M1, M2, which are characterized by a constant M^2, fall within this class since $M^{2\prime} = 0$. For models not belonging to this category the condition $M_0^{2\prime} \geq 0$ has to be checked as per case. Therefore when $M_0^{2\prime} \geq 0$ we have $\dot{V}(t_0) > 0$ and t_0 lies in the region the inflaton accelerates before its velocity vanishes for the first time. This occurs for times larger than $t_{\rm acc}$. Concluding, there is a broad class of models, those with $M_0^{2\prime} \geq 0$, for which the time ordering is $t_{\rm acc} < t_0 < t_1$. The situation is shown in Fig. 2.

Concerning the evolution of ϵ_1, it initially has a very small positive value and then starts increasing. This vanishes for first time when the velocity does, as is evident from Eq. (28), that is at time t_1. Therefore it ought to develop a maximum at some intermediate time, say $t_{\rm max}$ which is prior to t_1, i.e., $t_{\rm max} < t_1$. Whether $t_{\rm max}$ lies before or after t_0 we do not know as yet. We shall show that in the class of minimally coupled models M1, and also models M2, $t_0 < t_{\rm max}$ so that time ordering is as $t_0 < t_{\rm max} < t_1$. That is the minimum of the potential is reached for first time before ϵ_1 attains its first maximum, and later, at time t_1, ϵ_1 vanishes for first time along with velocity V. The proof relies on what is the sign of $\mathcal{N}$ in Eq. (30) at t_0. Since the potential and its derivative vanish at t_0, due to the fact that at this time $\phi = h = 0$, the value of $\mathcal{N}$ is

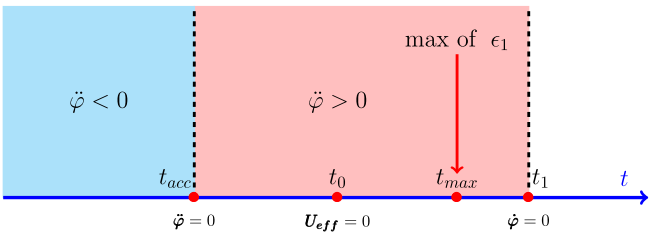

FIG. 2. The ordering of times $t_{\rm acc}, t_0, t_1$ is as depicted in this figure for a wide class of models, including those with $M^2 =$ constant. Between $t_{\rm acc}$ and t_1 the acceleration of inflaton ϕ is positive.

$$\mathcal{N}_0 = \mathcal{N}|_{t_0} = -\frac{V^5}{2}\left(\dot{V}R + \frac{R'}{2}V^2\right)\Big|_{t_0}. \tag{35}$$

From this it is seen that the sign of $\mathcal{N}_0$ follows that of the bracketed quantity in Eq. (35), due to the fact that $V(t_0) < 0$. Recall that velocity is negative for $t < t_1$ and t_0, i.e., earlier than t_1 as we have shown before. Therefore for the sign of $\mathcal{N}_0$ we need to study the acceleration and also R' at t_0. For the models M1, M2 the acceleration is positive at the point t_0, as we have already shown (see also Fig. 2). For these models, on account of Eq. (33), $R'(t_0)$ vanishes forcing the acceleration $\dot{V}(t_0)$ at t_0 to be positive, as we have already discussed. Therefore from (35) we have that $\mathcal{N}_0 > 0$. This entails that $\dot{\epsilon}_1(t_0) > 0$, using Eq. (29). Since ϵ_1 is monotonically increasing until this reaches its maximum at $t_{\rm max}$, positivity of $\dot{\epsilon}_1(t_0)$ states that the maximum of ϵ_1 is reached later than t_0, i.e., $t_0 < t_{\rm max}$, in the class of models having $M^2 =$ constant, as shown on Fig. 2. In the same figure the location of $t_{\rm max}$ relative to other critical times in the models M1, M2 is also shown. As we have stated, this covers the class of minimally coupled models, but also nonminimally coupled models in which $g(h)$, designating the coupling of the Ricci term in (8), is not constant.

Concerning the maximum value of ϵ_1 cannot exceed 3. In fact from (28) we have, writing explicitly the density ρ,

$$\epsilon_1 = 3\frac{V^2 + RV^4}{V^2 + (3R/2)V^4 + 2U_{\rm eff}}\text{`} \leq 3\frac{V^2 + RV^4}{V^2 + (3R/2)V^4} < 3, \tag{36}$$

therefore a strict upper bound on ϵ_1 can be established. At the time t_0 we have, due to the fact that the potential vanishes,

$$\epsilon_1(t_0) = 3\frac{1 + R_0V_0^2}{1 + (3R_0/2)V_0^2} \geq 2, \tag{37}$$

where the subscript 0 means evaluation at t_0. This lower bound on the value of $\epsilon_1(t_0)$ combined with the fact that ϵ_1 is monotonically increasing for all times $t \leq t_{\rm max}$ ensures that there is certainly a time $t_{\rm end} < t_0$ at which inflation ends, that is $\epsilon_1(t_{\rm end}) = 1$. This behavior is exemplified in Fig. 3 for a model in which $M^2 \equiv 1/3\alpha$ and $g(h) = 1$, and quadratic potential $V(h) = \frac{m^2h^2}{2}$. The values of the arbitrary parameters are $\alpha = 10^8$ and $m = 6.5 \times 10^{-5}$.

The results reached in this section are useful in our numerical treatment, in order to locate with the required precision the end of inflation, in models with $M^2 = 1/3\alpha$, especially when the parameter α is large. It is in these cases that inflaton dynamics cannot be described by slow-roll and the speed of sound, as we shall see, deviates from unity. This is equivalent to having non-negligible contributions

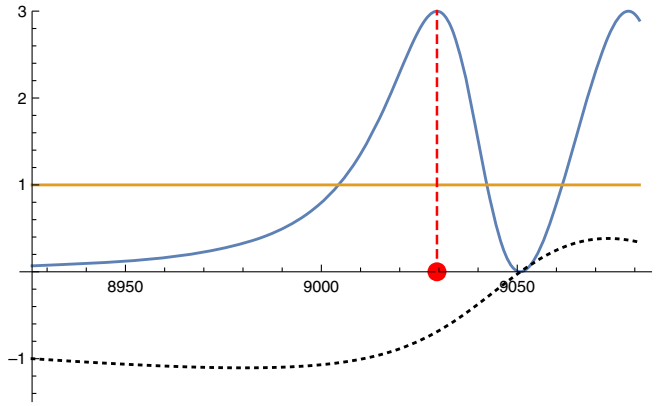

FIG. 3. In model I, and for $\alpha = 10^8$, we display the evolution of ϵ_1, in blue, and the velocity $\dot{\phi}$, dashed line, from some initial $t_{\rm ini}$ time. The horizontal axis is the rescaled cosmological time $t/\sqrt{\alpha}$, and the velocity is actually $\dot{\phi}$ divided by its values at $t_{\rm ini}$. The horizontal amber line crosses the ϵ_1 curve at where inflation ends, and this is prior to the minimum of the potential, whose location is shown by the red circle. The maximum of ϵ_1 lies to the right of the minimum, but it is hardly visible on the figure. ϵ_1 vanishes for first time after the minimum is reached. Its oscillatory behavior after is due to the fact that the velocity oscillates, after inflaton passes the minimum of potential.

from the quartic in the velocity L terms appearing in the action, as inflaton approaches the end of inflation.

V. UNIVERSE'S REHEATING TEMPERATURE

The reheating temperature of the Universe reached after its thermalization has been extensively studied and various mechanisms and models have been put under theoretical scrutiny [96,100–135]. Reheating in the framework of the Palatini gravity has been also studied in [44,51,56,67,73].

As for the number of e-folds left, $N_k = \ln\frac{a_{\rm end}}{a}$, from time some scale k crossed the sound horizon to the end of inflation is given in [136,137]. See also Refs. [108,124]. Note that the dependence on speed of sound c_s should be included in N_k, due to the fact that it may deviate from unity, as is the case in K-inflation models.

The number of e-folds accrued during the reheating period, $\Delta N_{\rm reh}$, is given by

$$\Delta N_{\rm reh} \equiv \ln\frac{a_{\rm reh}}{a_{\rm end}} = -\frac{1}{3(1+w)}\ln\frac{\rho_{\rm reh}}{\rho_{\rm end}}. \tag{38}$$

The subscripts (reh), (end) in the cosmic scale factor and the energy densities denote that these quantities are evaluated at the end of the reheating period and inflation, respectively. In terms of Hubble rate $\rho_{\rm end} = 3m_P^2 H_{\rm end}$, and therefore this is known once $t_{\rm end}$, or the values of the fields and their velocities at end of inflation, are known.

The effective equation of state parameter w in the reheating period, is the average

$$w = \frac{1}{\Delta N_{\rm reh}}\int_{N_{\rm end}}^{N_{\rm reh}} w(N)dN. \tag{39}$$

The integration variable is the number of e-folds and $\Delta N_{\rm reh} = N_{\rm reh} - N_{\rm end}$, where $N_{\rm end}, N_{\rm reh}$, are the number of e-folds at end of inflation and reheating periods, respectively. At the end of inflation $w(N_{\rm end}) = -1/3$, while $w(N_{\rm reh}) = 1/3$ corresponding to the onset of radiation dominance. Lacking a particular reheating mechanism the value of w is largely unknown, therefore we shall consider it as a free parameter taking values within some sensible range. In the canonical reheating scenario $w = 0$, but values in the range $\simeq$0.0–0.25, or larger, right after inflation, are also possible in some models [81,110,123,124].

In terms of $\Delta N_{\rm reh}$, for given w, one has for the reheating temperature, see, for instance, [116],

$$T_{\rm reh} = \left(\frac{30}{\pi^2}\frac{\rho_{\rm end}}{g^{*({\rm reh})}}\right)^{1/4}\exp\left(-\frac{3(1+w)\Delta N_{\rm reh}}{4}\right). \tag{40}$$

In our numerical studies we adopt the common values $g^{*({\rm reh})} = g_s^{*({\rm reh})} = 106.75$, corresponding to the SM content, as discussed before, for temperatures above $\sim$1 TeV.[6] Note that since $a_{\rm reh} > a_{\rm end}$ we have that $\Delta N_{\rm reh} \geq 0$, and therefore due to $w > -1$ the reheating temperature $T_{\rm reh}$ is bounded from above

$$T_{\rm reh} \leq \left(\frac{30}{\pi^2}\frac{\rho_{\rm end}}{g^{*({\rm reh})}}\right)^{1/4}. \tag{41}$$

The bound on the right-hand side of this defines the instantaneous reheating temperature, $T_{\rm ins}$. The temperature $T_{\rm reh}$ reaches this upper bound when the reheating process is instantaneous, in which case $\Delta N_{\rm reh} = 0$. Note that for rapid thermalization we have $\rho_{\rm end} = \rho_{\rm reh}$, from Eq. (38). The reheating temperature should be larger than $\sim$1 MeV so that big bang nucleosynthesis (BBN) is not upset. Lower values on $T_{\rm reh}$ have been established in [105] and more recently in [126].

The maximum reheating temperature depends, as we shall see, on the value of the sound of speed parameter c_s at end of inflation. This is not unity, in general, due to the fact that in the Palatini formulation of $\mathcal{R}^2$ gravity higher in the velocity $\dot{h}$ terms are unavoidable. In fact c_s is defined by

$$c_s^2 = \frac{\partial p/\partial X}{\partial \rho/\partial X}, \tag{42}$$

where X, defined after Eq. (13), is half the velocity squared. In terms of the fields h, or ϕ, and their velocities u and v, respectively, this receives the form

[6] With $g^{*({\rm reh})} = 100$ Eq. (40) coincides with that given in [116].

$$c_s^2 = \frac{1 + Lu^2/K}{1 + 3Lu^2/K} = \frac{1 + Rv^2}{1 + 3Rv^2}. \tag{43}$$

Inverting this we get

$$\omega = \frac{1 - c_s^2}{3c_s^2 - 1}, \tag{44}$$

where $\omega = Lu^2/K$, which is also equivalent to $\omega = Rv^2$. Actually ω is the same combination that appears in the equation of motion for the field h, or ϕ, respectively. The velocity c_s is thus controlled by ω, and it is seen from (43) that c_s^2 is strictly less than unity and approaches unity only when $\omega \ll 1$. Interestingly enough is also bounded from below by $1/3$. Thus c_s^2 takes values in the range

$$\frac{1}{3} < c_s^2 \leq 1. \tag{45}$$

These are strict mathematical bounds. The value of c_s^2 at any epoch is known if one solves the pertinent differential equation for h, or, equivalently, ϕ. The upper bound is reached for vanishing values of Lu^2/K, or Rv^2, and the lower limit when these quantities get values much larger than unity. As we shall prove the value of c_s^2 when inflation ends determines $\rho_{\rm end}$, and as a consequence the maximum reheating temperature.

At end of inflation $\rho + 3p = 0$ and the solution of this equation relates the velocity and the position at the end of inflation through Eq. (27), which in terms of the velocity of the field h takes the form

$$u^2(h) = \frac{2K}{3L}\left(-1 + \sqrt{1 + \frac{3LU_{\rm eff}}{K^2}}\right). \tag{46}$$

Both (27), or (46), hold at the end of inflation and cannot be treated analytically. Only numerically we can solve the pertinent differential equations and through these determine the end of inflation time, or equivalently the value of the position at end of inflation. Approximate solutions do exist but they are unreliable, in the present case, due to the presence of the L-dependent terms. As we have already discussed, and depending on the values of the parameters involved, the solutions may differ substantially from slow-roll towards end of inflation. Therefore evaluation of end of inflation period using approximations, relying on the use of the slow-roll parameters ϵ_V, η_V, poorly determine when the end of inflation actually occurred.

Using the expression for the density ρ one can use (27), (46), to find

$$\rho_{\rm end} = \left.\frac{3}{2R}\omega(1+\omega)\right|_{\rm end}. \tag{47}$$

In this, ω has been defined previously and in terms of the sound of speed is given by Eq. (44).[7]

Note that all quantities in (47) are meant at the end of inflation. Combining these we find

$$\rho_{\rm end} = \left.\frac{3}{R}\frac{(1 - c_s^2)c_s^2}{(3c_s^2 - 1)^2}\right|_{\rm end}. \tag{48}$$

However, the ratio $R = \frac{L}{K^2}$ can be expressed in terms of the potential, using (15), from which using the Eqs. (27), or (46), we finally get

$$\rho_{\rm end} = \left.\frac{9M^2}{4}(1 - c_s^2)\right|_{\rm end}, \tag{49}$$

a very handy relation. Note that all quantities are evaluated at the end of inflation. Using the lower bounds on c_s^2, see Ref. (45), we get a strict upper bound on $\rho_{\rm end}$,

$$\rho_{\rm end} < \left.\frac{3M^2}{2}\right|_{\rm end}. \tag{50}$$

In Eqs. (49) and (50) the quantity M^2 is not constant, in general, but a function of the position, h (or ϕ), which should be replaced by its end of inflation value, as well. The actual upper bounds, which are extracted by solving the pertinent differential equations numerically, may be smaller than those of Eq. (50). In fact c_s^2, at the end of inflation, depending on the model and the values of the parameters involved, may be close to unity. This is indeed the case when the effect of the L terms is small throughout the inflation evolution. It may also happen that the lower bound in (45) may be larger due to the fact that $L\dot{h}^2/K$ can never exceed some critical value. In that particular case the upper bound (50) is lowered. This is the case, for instance, in the minimally coupled models to be discussed below.

In general, there is a critical time, say $t_{\rm crit}$, for which $\ddot{h} = 0$, that is the acceleration of h vanishes. Note that this does not imply that the corresponding acceleration for the field ϕ vanishes at $t_{\rm crit}$.[8] From initial stage of inflation until $t_{\rm crit}$ the acceleration, and also the velocity, of h are negative, $\ddot{h} \leq 0$, $\dot{h} < 0$. Therefore in this time interval a solution of (17) exists provided,

[7]Obviously (47) holds provided ω, as defined by Eq. (44), is nonvanishing. The $\omega = 0$ case corresponds to $R = 0$, and hence $c_s^2 = 1$ which is the case in the usual inflation scenarios. In this case it is well known that $\rho_{\rm end} = \frac{3}{2}U_{\rm eff}$ at the end of inflation.

[8]In fact when $\ddot{h} = 0$ we have,

$$\ddot{\phi} = \frac{1}{2K}\frac{dK}{d\phi}\dot{\phi}^2 \neq 0. \tag{51}$$

$$S_{\rm crit} \equiv U'_{\rm eff}(h) + \frac{1}{4}(2K' + 3L'\dot{h}^2)\dot{h}^2 \geq 0. \tag{52}$$

This puts an upper bound on the velocity $\dot{h}$ if $L' < 0$ which is indeed the case in a variety of models. This is exemplified below for a class of models that have attracted much interest.

A. Minimally coupled h^n models

These models belong to the class **M1**, discussed previously, characterized by constants g and M^2, and a potential $V(h)$ which is a monomial,

$$g = 1, \qquad M^2 = 1/3\alpha, \qquad V(h) = \frac{\lambda}{n}h^n \quad (n = \text{positive integer}). \tag{53}$$

Then the functions K, L are given by

$$K(h) = (1 + ch^n)^{-1}, \qquad L = \alpha K, \tag{54}$$

with the constant c being defined by

$$c = \frac{4\lambda\alpha}{n}. \tag{55}$$

The case $n = 2$ belongs to the class of the cosmological attractors [138,139], which is clearly seen if one uses the canonically normalized field ϕ of (18), see Ref. [32]. Thus L is linearly dependent on K through the constant parameter α. The potential $U_{\rm eff}$ is given by

$$U_{\rm eff}(h) = \frac{1}{4\alpha}\frac{ch^n}{1 + ch^n} = \frac{1}{4\alpha}(1 - K). \tag{56}$$

In this model the terms $S_{\rm crit}$, defined in (52), receive the form

$$S_{\rm crit} = U'_{\rm eff}(h)(1 - 2\alpha\dot{h}^2 - 3(\alpha\dot{h}^2)^2). \tag{57}$$

Due to the fact that the derivative of the potential stays positive until h vanishes for first time, at t_0, positivity of $S_{\rm crit}$, in the interval $t \leq t_{\rm crit}$, entails

$$\alpha\dot{h}^2 < \frac{1}{3}, \tag{58}$$

which surely applies at $t_{\rm crit}$. Since at $t_{\rm crit}$, where $\ddot{h} = 0$, the velocity gets its minimum value, and it is negative until it vanishes for the first time at t_1, we have,

$$\dot{h}(t) > -\frac{1}{\sqrt{3\alpha}}, \quad \text{or} \quad u(h) > -\frac{1}{\sqrt{3\alpha}}, \tag{59}$$

from the beginning of inflation until the velocity vanishes for the first time. This region includes the whole inflationary period and therefore these bounds apply to the end of inflation. Whether the lower bound above is reached in the inflationary era depends on inputs. Using (46) and the bound (59) one can derive

$$h^n_{\rm end} \leq \frac{5}{3c}, \tag{60}$$

in this class of models. For large α, corresponding to large c, when λ is fixed, the end of inflation value $h_{\rm end}$, is small due to (60). Note that the bound (59) yields a more stringent lower bound on c_s^2 than the one given by Eq. (45). In fact one has, using (43),

$$c_s^2 > \frac{2}{3}, \tag{61}$$

which on account of (49) results to

$$\rho_{\rm end} < \frac{3M^2}{4} = \frac{1}{4\alpha}, \tag{62}$$

which is actually half of the bound given by (50). As we have already stated the actual upper bound is even less and depends on the precise value of c_s^2 at the end of inflation. The right-hand side of (62) sets the maximum value the energy density $\rho_{\rm end}$ can reach. Obviously, this is almost saturated if $c_s^2 \simeq \frac{2}{3}$ at the end of inflation, which using (44), yields $Rv^2 \simeq 1/3$, or $\alpha u(h)^2 \simeq 1/3$. That is, at end of inflation the velocity of the h-field should be close to its lowest bound, as this is set by Eq. (59), for the energy density to reach its maximum allowed value in this type of model. Then knowing the velocity at the end of inflation, one can use (27), or same (46), to derive the value of $h_{\rm end}$. This is found to approach its upper bound (60), $h^n_{\rm end} \simeq \frac{5}{3c}$. For large values of the parameter α this is indeed the case in these types of models. That is, the bounds derived previously are saturated for sufficiently large values of α. This will be exemplified in the following, when discussing the bounds set on the reheating temperature.

The aforementioned bound on $\rho_{\rm end}$ yields in turn bounds for the instantaneous reheating temperature $T_{\rm ins}$ which is the largest reheating temperature allowed in any inflation model. From Eq. (41) we actually have

$$T_{\rm ins} = \left(\frac{30}{\pi^2}\frac{\rho_{\rm end}}{g^{*(\rm reh)}}\right)^{1/4} \leq \left(\frac{15}{2\pi^2 g^{*(\rm reh)}}\right)^{1/4}\alpha^{-1/4}. \tag{63}$$

To convert it to GeV this should be multiplied by the reduced Planck mass $m_P = (8\pi G_N)^{-1/2} \simeq 2.435 \times 10^{18}$ GeV. With $g^{*(\rm reh)} = 106.75$ this yields the bound

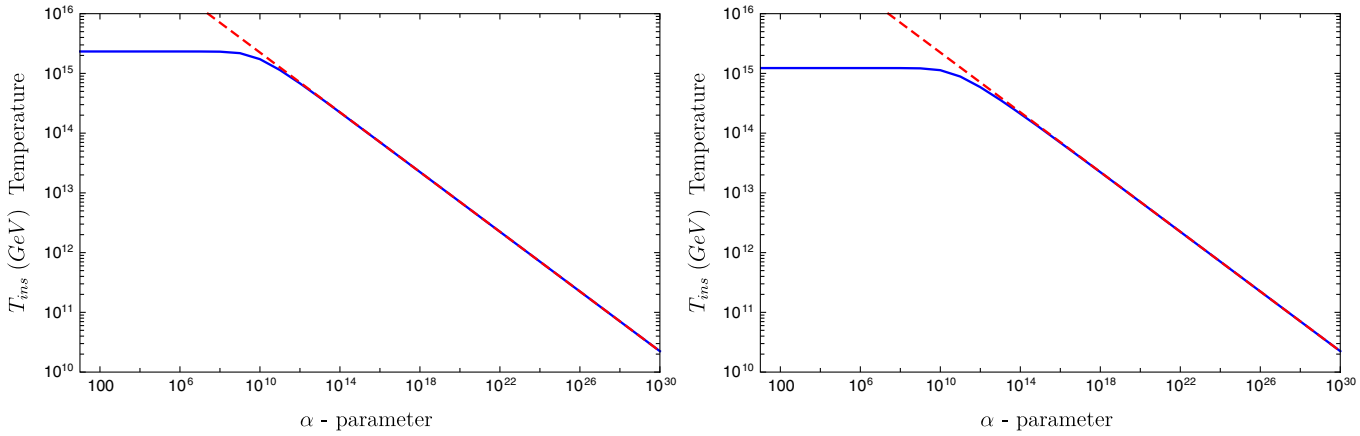

FIG. 4. On the left, we display the bound set on the instantaneous reheating temperature as a function of α for the minimally coupled model with potential $V(h) = m^2h^2/2$ and $m = 6.2 \times 10^{-6}$. On the right we show the same bound for the quartic potential $V(h) = \lambda h^4/4$ and $\lambda = 2.025 \times 10^{-13}$. In both figures, the solid (blue) line is the actual bound as derived numerically and the dashed red line is the bound of Eq. (64). These coincide when α exceeds $\sim 10^{10}$.

$$T_{\rm ins} \leq \frac{0.290 \times m_P}{\alpha^{1/4}} = \frac{0.7073 \times 10^{18}}{\alpha^{1/4}}\ \text{GeV}. \quad (64)$$

In Fig. 4 we display the actual upper bound on $T_{\rm ins}$ (blue solid line), derived numerically, and the strict mathematical upper bound of Eq. (64), (dashed red line), which is based on (62). The cases displayed correspond to the minimally coupled model with $n = 2$ (left pane), with the parameter λ of the scalar potential in Eq. (53) given by $\lambda \equiv m^2$, with $m = 6.2 \times 10^{-6}$, and the case $n = 4$ (right pane), corresponding to $\lambda = 2.025 \times 10^{-13}$. These values are consistent with scalar perturbations, as we shall see.

Note that when $\alpha \lesssim 10^{10}$ the actual bound is lower than the mathematical upper bound set on $T_{\rm ins}$ and is almost independent of α, depending, however, on the values of m or λ. However, the two bounds coincide for values $\alpha > 10^{10}$. The reason is that in this region of α the sound of speed squared c_s^2, at the end of inflation, approaches $2/3$, as we have already discussed, and the velocity approaches its lowest allowed limit, as this is set by (59), resulting in $\rho_{\rm end} \simeq 1/4\alpha$. Note that in this case the contribution of the L terms is important in extracting the correct value of the field h at the end of inflation, $h_{\rm rend}$, and hence the correct values for $\rho_{\rm end}$. In the regime of small α, smaller than 10^{10} or so, the sound of speed squared c_s^2 at the end of inflation, is very close to unity, that is the contribution of the L terms is indeed negligible and the dynamics is the same as in ordinary models; that is, models which quartic in the velocity terms are absent. It is only in this case that the usual slow-roll approximation schemes for extracting $h_{\rm rend}$ can be employed.

The CMB observations restrict considerably the predictions of all inflationary models. The first calculations were performed in [140–142] and since then there has been intense activity towards improving the calculations, by considering also higher order corrections, demanded by the precise measurements of the cosmological parameters, or tackle theories with variable speed of sound [91,143–159]. Therefore the bounds discussed previously on the instantaneous reheating temperature are narrowed if the observational constraints, from various astrophysical sources are used. These actually impose bounds on the parameter α, or, equivalently, on the scale of inflation. For the derivation of the cosmological parameters, we shall make use of the number of e-folds N_*, corresponding to a pivot scale k^*, which can be written as [136,137],

$$N_* = 66.89 - \ln c_s^* - \ln\left(\frac{k^*}{a_0 H_0}\right) + \frac{1}{4}\left(\ln\frac{3H_*^2}{m_P^2} + \ln\frac{3H_*^2 m_P^2}{\rho_{\rm end}}\right) - \frac{1}{12}\ln g_s^{*(\rm reh)} + \frac{1-3w}{12(1+w)}\ln\left(\frac{\rho_{\rm reh}}{\rho_{\rm end}}\right). \quad (65)$$

See also Refs. [108,124]. The advantage of using this, among others, is that it incorporates information on the reheating temperature through the last term, the so-called *reheating parameter*. This does not contribute when reheating is instantaneous, in which case $\rho_{\rm reh} = \rho_{\rm end}$. It does not contribute either when $w = 1/3$, a well-known result. We have included in Eq. (65) the dependence on the variable speed of sound and the reduced Hubble parameter is taken equal to $h = 0.676$, for details see Ref. [51]. Given a pivot scale k^* the end of inflation affects the N^* through $\rho_{\rm end}$. Note that in our approach we solve numerically the pertinent background equations, to find the values of the cosmic scale factor and inflaton velocity, as functions of the field values, and we use (27), or (46), to find where inflation ends. To this goal slow-roll approximation has not been invoked. In the sequel we solve (65) to find the pivot

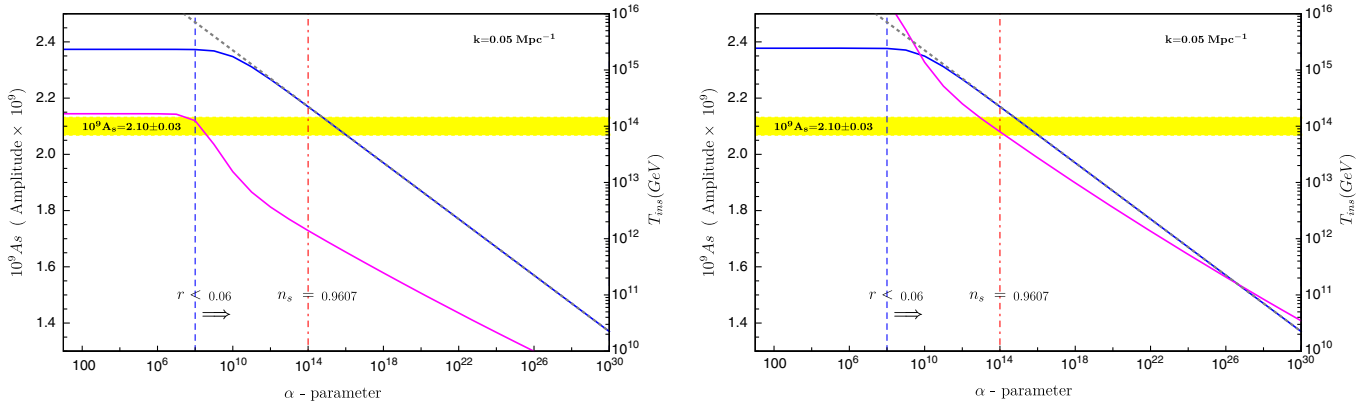

FIG. 5. The bound set on the instantaneous reheating temperature, and other observables, as a function of α for the minimally coupled model with potential $V(h) = m^2h^2/2$, for $m = 6.2 \times 10^{-6}$ (left) and $m = 6.8 \times 10^{-6}$ (right). In these figures, we display the amplitude of scalar perturbations A_s, in magenta, with values on the left vertical axis, as a function of the parameter α, for k^* shown in the figure, assuming instantaneous reheating, $T_{\rm ins}$, drawn in a solid blue line, with values shown on the right vertical axis. The horizontal stripe (in yellow) marks the region allowed by Planck 2018 observations on A_s. Along we show the lower observational bound on the spectral index n_s, red dash-dotted vertical line, and the bound $r < 0.06$ set on the tensor to scalar ratio, blue dashed line, in each of the figures.

values, ϕ^*, corresponding to the first horizon crossing of the given scale k^*, through which the cosmological parameters are determined. In the slow-roll approximation this is implemented by using $N^* = \int_{\phi_{\rm end}}^{\phi^*} \frac{U d\phi}{U'}$, where U is the inflaton potential. Concerning the cosmological observables, for a pivot scale k^* that exited the sound horizon at t^*, that is, $k^* c_s(t^*) = a(t^*)H(t^*)$, the scalar and tensor power spectra can be expanded about this pivot. Keeping the first order terms in the Hubble flow functions (HFF), one has that the corresponding amplitudes are given by

$$A_s = \frac{H_*^2}{8\pi^2 m_P^2 \epsilon_1^* c_s^*}(1 - 2(D+1)\epsilon_1^* - D\epsilon_2^* - (2+D)s_1^*),$$
$$A_t = \frac{2H_*^2}{\pi^2 m_P^2}(1 - 2(D + 1 - \ln c_s^*)\epsilon_1^*). \tag{66}$$

These can be found in [157], where techniques similar to the WKB approximation have been used for their derivation. The constant D is given by $D = 7/19 - \ln 3$. From these one has for the tensor-to-scalar ratio,

$$r \equiv \frac{A_t}{A_s} = 16\epsilon_1^* c_s^*(1 + 2\ln c_s^* \epsilon_1^* + D\epsilon_2^* + (2+D)s_1^*). \tag{67}$$

Concerning the spectral index, following standard definitions, to the same approximation, we have

$$n_s = 1 - 2\epsilon_1^* - \epsilon_2^* - s_1^*. \tag{68}$$

In the equations given before ϵ_2, s_1, whenever they appear, are given by $\epsilon_2 = \dot{\epsilon}_1/\epsilon_1 H$ and $s_1 = \dot{c}_s/c_s H$. For the primordial power spectrum we consider scales k sampled by Planck CMB observations, lying in the range $\sim 10^{-3}$–10^{-1} Mpc^{-1}. The spectrum features small amplitudes $A_s \sim 10^{-9}$ and is almost scale invariant.[9]

In Fig. 5, we display the instantaneous temperature $T_{\rm ins}$ and the bounds set by other observables, assuming that reheating is instantaneous, that is $T_{\rm reh} = T_{\rm ins}$. This is drawn in the solid blue line with values shown on the right vertical axis. The gray dashed line is the bound on the instantaneous temperature discussed previously, see Fig. 4. These figures are the predictions for the minimally coupled model with potential $V(h) = m^2h^2/2$, and slightly different values $m = 6.2 \times 10^{-6}$ (left panel) and $m = 6.8 \times 10^{-6}$ (right pane). In these figures, the amplitude of scalar perturbations A_s is displayed (in magenta) as a function of the parameter α, with values shown on the left vertical axis, for a pivot scale $k^* = 0.05$ Mpc^{-1}. The horizontal stripe, in yellow, marks the region allowed by Planck 2018 observations on $A_s = (2.10 \pm 0.03) \times 10^{-9}$, [84,85]. One notices that A_s puts severe constraints on the parameter α, and hence on the instantaneous temperature as well, given the value of the parameter m.

Along we show the lower experimental bound on the spectral index n_s, as a red dash-dotted vertical line. The region to the left of this line is within the Planck 2018 limits $n_s = 0.9649 \pm 0.0042$. The bound $r < 0.06$ on the tensor to scalar ratio r, set by various measurements, is also shown as a vertical blue-dashed line. The allowed region by the r-bound stands to the right of this line, designated by an arrow. The aforementioned bound on r is pretty close to that established by Planck 2018 data, when combined with

[9]Starobinsky-type models in metric formulation, with nonminimal coupled scalar field, can yield enhanced primordial curvature perturbations on small scales [160]. Such a study is however outside the scope of this article.

the BICEP2/Keck Array BK15 measurements, see Refs. [85,86]. The BICEP/Keck Collaboration [87] has further put a more tightened bound $r < 0.036$. However, we shall prefer to use the more conservative bound $r < 0.06$. Actually using the bound $r < 0.036$ will shift very little the blue-dashed line to the right and therefore the predictions are almost intact.

The combined n_s, r bounds further narrow the range of α values allowed by A_s. We remark that these bounds, unlike those stemming from A_s, are rather insensitive to small changes of the parameter m and for this reason the location of the r and n_s bound are almost the same in the two figures. However A_s predictions depend sensitively on m. In the displayed figures the A_s curves have a quite different shape, although the parameter m has only slightly changed. Notice that the case $m = 6.8 \times 10^{-6}$, corresponding to the figure on the right, can be considered as the largest allowed by the A_s constraint, if the bound on n_s is observed, assuming instantaneous reheating. Actually for larger m values the allowed by A_s region lies to the right of the n_s lower observational limit, shown by the dashed-dotted red line in the figures, and hence excluded. On the other hand the case $m = 6.2 \times 10^{-6}$ is the minimum allowed, as lower values move the allowed A_s region to the left of the $r < 0.06$ bound. Therefore combining all bounds we have that the allowed window for m is in the range $m \simeq (6.2 - 6.8) \times 10^{-6}$ with corresponding limits for α in the range $\alpha \simeq 10^8$–10^{14}. These induce the bounds $T_{\rm ins} \simeq 2.2 \times 10^{14}$ and $T_{\rm ins} \simeq 2.3 \times 10^{15}$ GeV, respectively, with the larger (smaller) bound corresponding to the smaller (larger) allowed value of α. We remark that for m values in the range given before, most of the allowed α range, actually $\alpha > 10^{10}$, is within the regime where the quartic in the velocity terms are sizable and $c_s^2 \simeq 2/3$ at the end of inflation. Note, however, that the first horizon crossing of the CMB scales occurs when $c_s^2 \simeq 1$, that is when the quartic terms are negligible. Therefore, when $\alpha > 10^{10}$, the previously discussed bounds could not have been predicted in the usual slow-roll approximation schemes. In fact the inflaton leaves the slow-roll regime well before the end of inflation, for such high values of α. As a result, a more delicate study is needed in deriving the end of inflation energy density $\rho_{\rm end}$, which determines the instantaneous reheating temperature, which we do in the present work. It may not have been passed unnoticed that for $\alpha \lesssim 10^9$ the amplitude A_s, and also the temperature $T_{\rm ins}$, are insensitive to changes in α. This is due to the fact that for such values of α the quartic in the velocity terms are small and slow-roll is a good approximation scheme. Then using the slow-roll function ϵ_V to find the pivot value h^*, or ϕ^*, and end of inflation $h_{\rm end}$, or $\phi^*_{\rm end}$, yields results that are accurate enough. That done, one finds that $A_s, T_{\rm ins}$ depend explicitly on the parameter m and only implicitly on α. That was shown analytically in [51]. This is the reason for fixed m values these quantities are almost constant with changes in α. The same holds for other models, as well, namely, the Higgs model, which we shall discuss in the next section.

Therefore, in the framework of Palatini $\mathcal{R}^2$ inflation, in the context of the minimal models with monomial potential $V(h) = m^2h^2/2$, and $g = 1, M^2 = 1/3\alpha$, the scalar power spectrum amplitude A_s constrains the parameter m, which in conjunction with n_s, r data lead to bounds on α. Upper bounds on the instantaneous temperature can be established, which are saturated for large α. For such values of α need go beyond slow-roll to derive reliable cosmological predictions. Note that by reinstating units, the plateau values for the potential can be cast in the form $U_{\rm eff}(h) = 3M_s^2m_P^2/4$, for a comparison with Starobinsky inflation, where for the case at hand the inflation scale M_s is defined by $M_s = m_P/\sqrt{3\alpha}$. Then the previously discussed bounds on α translate to $M_s \simeq (10^{-4} - 10^{-7})m_P$. For comparison, recall that CMB amplitude restricts the Starobinsky scale to $M_s = M_{\rm Starobinsky} \simeq 1.3 \times 10^{-5}m_P$.

So far we have assumed that reheat is instantaneous and derived bounds arising from cosmological observations. By the same token, similar bounds can be also established for lower temperatures, as well. The analysis, in this case, depends on the effective equation of state parameter w. We shall assume that the latter takes values in the range $w \simeq 0.0$–0.25, with $w = 0$ corresponding to the canonical reheating scenario. This range of w is favored in some inflationary scenarios, as we have already discussed. For the minimally coupled model, with potential $V(h) = m^2h^2/2$, we have found that the bounds established for the parameter m, $6.2 \times 10^{-6} \lesssim m \lesssim 6.8 \times 10^{-6}$, hold for lower temperatures as well. Values outside this range are ruled out by the cosmological data. In fact lower m values lead to $10^9A_s \lesssim 2.0$, while for larger values, either A_s is small or, even when A_s is within observational limits, n_s is too low. Hence m values outside the aforementioned range are discarded. For any m, within this range, the amplitude A_s and/or r, the tensor to scalar ratio, put lower bounds on α, while upper bounds on α are set by A_s and/or n_s. Given the parameter m, a range of allowed α is therefore established, and for any α, in this range, the reheating temperature $T_{\rm reh}$ takes values within an interval whose lower/upper limits correspond to the minimum/maximum allowed A_s. These limits are larger (smaller) the larger (smaller) the value of α is, within its allowed range. This is exemplified in Fig. 6, where for the largest and smallest allowed values of m, $m_{\rm max} \simeq 6.8 \times 10^{-6}$ and $m_{\rm min} \simeq 6.2 \times 10^{-6}$, we have drawn the amplitude A_s, as function of the reheat temperature, for different values of the parameter α. Each line shown is marked by an integer which denotes the value of $\log_{10}\alpha$. The right end of each A_s line stops at the instantaneous reheating temperature. Whenever a star symbol appears on a line it is there to indicate the boundary $n_s = 0.9607$. On the other hand, whenever a red bullet appears it designates the location of

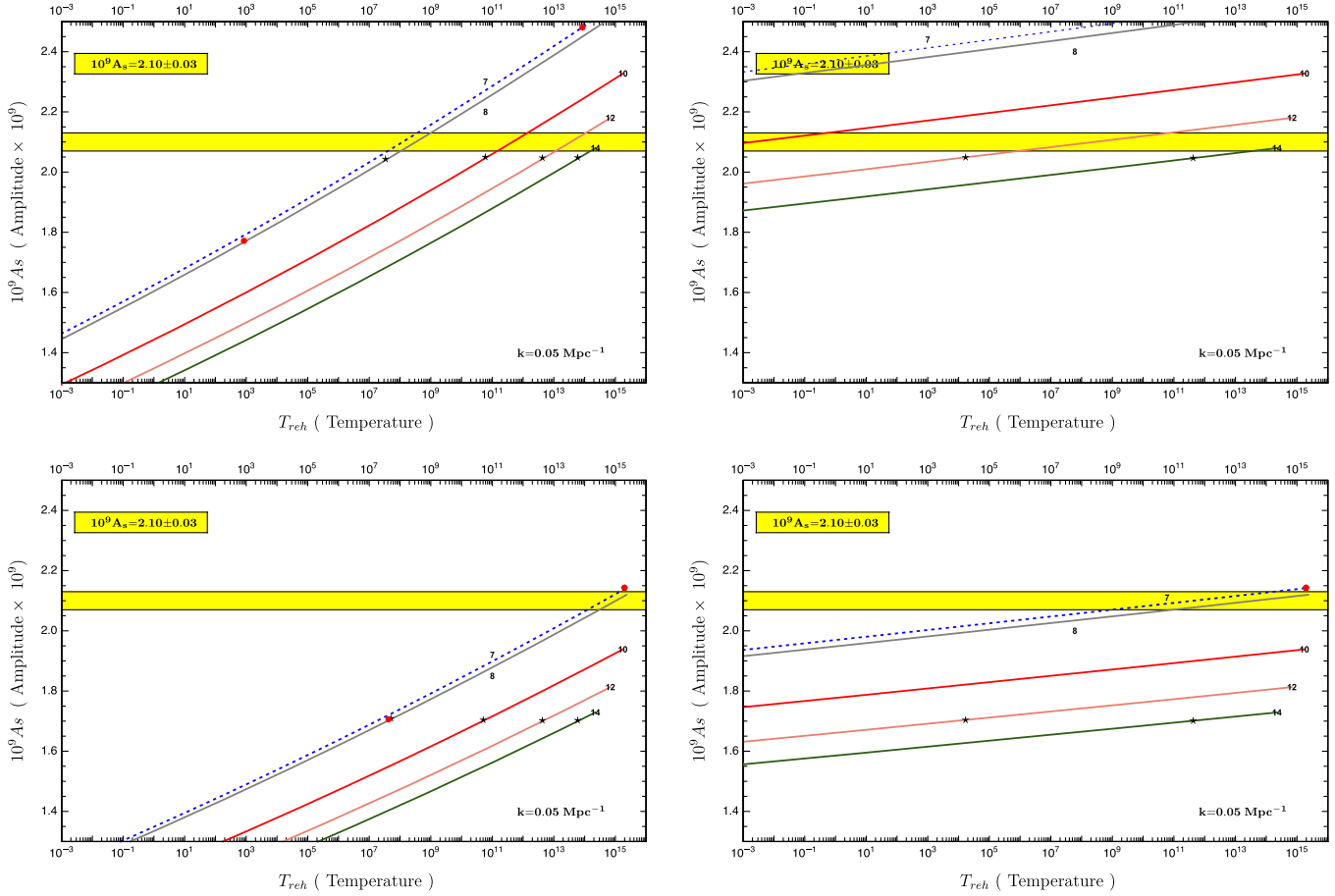

FIG. 6. The amplitude A_s as a function of the reheat temperature, for various values of α, marked by an integer on each line denoting the value of $\log_{10}\alpha$, for the minimally coupled model with potential $V = m^2h^2/2$. The equation of state parameter equals to $w = 0.0$, left pane, and $w = 0.25$, right pane. At top, the parameter m has its highest allowed value, $m = 6.8 \times 10^{-6}$ and at bottom m gets its lowest allowed value, $m = 6.2 \times 10^{-6}$. The star symbol, whenever it appears, indicates the point for which $n_s = 0.9607$, the lowest allowed observational bound. The red bullet, if it appears, marks the boundary $r = 0.06$. Points on the line lying to the left of these symbols are not allowed.

the upper bound $r = 0.06$. Points on the line lying to the left of these symbols are not acceptable. Whenever any of these symbols is absent there is no restriction stemming from the corresponding bound.

On the left panes of Fig. 6, the equation of state parameter is $w = 0.0$ and on the right panes $w = 0.25$. For each α, the segment of each line within the yellow stripe, which designates the allowed range $10^9 A_s = 2.10 \pm 0.03$, projected onto the $T_{\rm reh}$ axis locates the allowed range of temperatures for this value of α. For instance, for the case shown on the top left of this figure, when $\alpha = 10^{10}$ the temperature range is $\simeq 10^{11}$–10^{12} GeV. As far as values of α are concerned, for the same case, the allowed range of α is $\alpha \simeq 10^8$–10^{14}. Lower values are excluded since they violate the $r < 0.06$ bound. As a demonstration of it, we have displayed the $\alpha = 10^7$ case, by a blue dashed line, which while being in agreement with n_s data, and also A_s in some temperature range, the bound on r is violated for any temperature. This is indicated by the red bullet on the far right of it. The same holds for lower α values. Therefore only values $\alpha \gtrsim 10^8$ are allowed. For the figure at the bottom right, the allowed range is $\alpha \simeq 10^{10}$–10^{14}. Only values within this range can be compatible with A_s observational limits, as is clearly seen. Note that, although the α range has shrunk, in comparison with the $w = 0$ case, it allows for lower temperatures. This will be discussed in the sequel.

Concerning the highest temperature attainable, for any given value of the parameter m, there is always a narrow range of α's for which their corresponding instantaneous temperature are cosmologically acceptable, in the sense of giving predictions compatible with all data. See, for instance, Fig. 5. Since the instantaneous temperature $T_{\rm ins}$ drops with increasing α, the lowest of these α's, yields the larger $T_{\rm ins}$ for this particular value of m. On the other hand, the minimum value of the parameter m, $m_{\rm min} \simeq 6.2 \times 10^{-6}$, yields the lowest possible α. Therefore, applying this reasoning for the minimum $m = m_{\rm min}$, we pick the higher

possible instantaneous temperature which is the highest possible reheating temperature. Phrased differently, and with reference Fig. 6, for any given value of the parameter m the higher temperature is the instantaneous corresponding to the lowest α whose A_s line ends up within the yellow band $10^9 A_s = 2.10 \pm 0.03$, shown in the figure, provided all other available data are observed. Thus, the highest possible reheat temperature is the instantaneous corresponding to the minimum value, $m = m_{\min} \simeq 6.2 \times 10^{-6}$ and the lowest in this case α, having its A_s line ending inside the yellow stripe, satisfying, also, the n_s, r data. This is clearly shown at the bottom panes of Fig. 6 from which we see that the lowest α lies in a very narrow range around $\alpha \simeq 10^8$, yielding $T_{\rm ins} \simeq 2.30 \times 10^{15}$ GeV. This result is w independent, and for this reason the values of $T_{\rm ins}$ are the same for both left and right figures presented. Therefore the maximal attainable temperature within the context of this model is 2.30×10^{15} GeV, quoted before, as being the largest instantaneous temperature, of all, for which all data are satisfied. In order to complete the picture, for the maximum value $m_{\max} \simeq 6.8 \times 10^{-6}$ the situation is displayed at the top of Fig. 6. In this case the lowest allowed α, with the desired properties, is $\alpha \simeq 10^{14}$, or somehow lower than it. This yields as instantaneous temperature 2.23×10^{14} GeV, obviously lower than the one corresponding to $m_{\min}$ by an order of magnitude or so.

As far as the lowest temperatures are concerned. It should not have passes unnoticed that when $w = 0$, the available temperatures have lower bounds. From the left panes in Fig. 6, at both top and bottom, this is clearly seen, and this is the case for any allowed value of m in the canonical reheating scenario, i.e., when the equation of state parameter is vanishing. In the $w = 0$ case the lowest temperature is reached when m gets its maximum value. From the top left figure in Fig. 6, we see that this cannot be lower than $T_{\rm reh} \simeq 10^8$ GeV, obtained when $\alpha \simeq 10^8$, the minimum allowed. For the minimum m, the lowest temperature is higher, $T_{\rm reh} \simeq 10^{14}$ GeV, as seen at the left bottom figure. Thus in this model and for canonical reheat, lower bounds on $T_{\rm reh}$ are imposed, and temperatures below $T_{\rm reh} \simeq 10^8$ GeV are unattainable. However the situation drastically changes if w is allowed to take nonvanishing values. For $w = 0.25$ and for the maximum m, at the top right panel of figure, the lowest acceptable α is $\simeq 10^{10}$, and temperatures in the range $\simeq 0.01$ MeV–0.6 GeV are allowed.[10] Recall, however, that low temperatures are constrained by BBN, which imposes lower bounds $\simeq 1$ MeV on the reheating temperature. For the minimum m case; see right pane at bottom, lower temperatures, as compared to $w = 0$, can be obtained but not lower than $\simeq 10^{11}$ GeV.

[10]As a general remark, concerning w, the closer the w is to the radiation value $1/3$ the more extended is the range of the allowed temperatures. Evidently, for $w = 1/3$, there are no restrictions imposed on the reheat temperature.

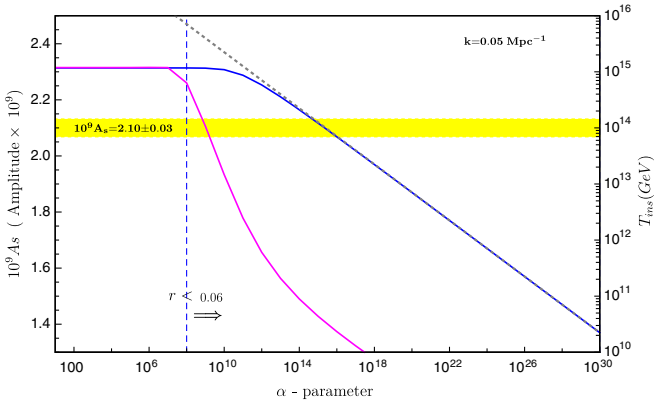

FIG. 7. The bound set on the instantaneous reheating temperature, and other observables as a function of α for the minimally coupled model with potential $V(h) = \lambda h^4/2$, for $\lambda \equiv m^2$ with $m = 4.1 \times 10^{-7}$. Along we show the bound $r < 0.06$ set on the tensor to scalar ratio, as a blue dashed line. In the whole range for α the spectral index is below observational limits.

For the minimally coupled model with quartic potential $V(h) = \lambda h^4/2$ the situation is similar as far as A_s and r constraints are concerned. However there is no agreement with n_s data. As an example we display a representative case, in Fig. 7, for $\lambda \equiv m^2$ with $m = 4.1 \times 10^{-7}$. As in the $V(h) = m^2 h^2/2$ case there is a lower bound on $\alpha > 10^8$, imposed by $r < 0.06$, and for the case displayed there is also complete agreement with the amplitude A_s for α slightly below 10^{10}. However the spectral index for any α, allowed by A_s, is $n_s < 0.9490$, well below the observational limits. Therefore the quartic potential fails to satisfy all observational data. The situation changes if the model is promoted to include nonminimal couplings, as is the case of the Higgs model to be studied in the next section.

B. Nonminimally coupled models

A particularly interesting model, belonging to the class **M2**, is the one for which

$$g = 1 + \xi h^2, \qquad M^2 = 1/3\alpha, \qquad V(h) = \frac{\lambda}{4} h^4. \tag{69}$$

This model is well known to arise from the Higgs coupling to Palatini gravity in the unitary gauge when the electroweak scale is considered small. The parameter ξ sets the coupling of the Higgs field to the curvature terms and α is the coefficient of the quadratic in the curvature term as defined in (8).

The Higgs coupling to gravity and its role as the inflaton, in the metric formulation, has been proposed in [161,162] and it has been widely studied since then in Refs. [29,32,33,36,38,44,45,51,55,61,63,67,68,75,78,81,83,128,131,163–188] both in the context of the metric and Palatini formulation. The importance of the $\mathcal{R}^2$ coupling, in the Palatini approach, has been discussed

in [32,33,36,38,51,55,61,67,68,75,187]. Quintessential inflation in the framework of Palatini $\mathcal{R}^2$ gravity has been considered in [79,80,82].

In this work we shall show that the quartic coupling λ, as in the minimally coupled quartic model studied previously, is constrained considerably by cosmological data, especially by the power spectrum amplitude A_s. Combining all data, further limits are imposed restricting the available options. The pertinent functions K, L are given by

$$K(h) = \frac{1+\xi h^2}{(1+\xi h^2)^2 + ch^4}, \qquad L = \frac{\alpha}{(1+\xi h^2)^2 + ch^4}, \tag{70}$$

while the potential $U_{\rm eff}$ is given by

$$U_{\rm eff}(h) = \frac{1}{4\alpha}\frac{ch^4}{(1+\xi h^2)^2 + ch^4}. \tag{71}$$

The bounds set on the instantaneous temperature are more difficult to derive in this case due to the dependence on the parameter ξ. Although the analysis is the same, in this case the term in Eq. (52) is not as simple as that given by (57). For the case at hand we had better used $\omega = L\dot{h}^2/K$ as dependent variable n Eq. (20), instead of u. Thus is the same quantity used in Eq. (44). That done the pertinent equation takes on the form

$$(1+3\omega)\frac{d\omega}{dh} - 3H\sqrt{\frac{4L}{K}}(1+\omega)\omega^{1/2} + \tilde{S}_{\rm crit} = 0, \tag{72}$$

where

$$\tilde{S}_{\rm crit} = \frac{2L}{K^2}U'_{\rm eff}(h)(1-2\omega-3\omega^2). \tag{73}$$

Modulo the factor $2L/K^2$, this is reminiscent of (57). In (72) we have anticipated the fact that in the region of interest, from beginning of inflation until the velocity u vanishes for the first time, u is negative, and hence the negative sign in the Hubble term. Note that ω starts increasing, as h decreases, while it vanishes when the velocity u vanishes for the first time, and therefore a maximum of $\omega_{\rm max}$ is developed at a critical value $h_{\rm crit}$. At this point $d\omega/dh = 0$, while $d\omega/dh \leq 0$ for any $h \geq h_{\rm crit}$, since ω increases with decreasing h, in this region. Therefore from (72) we deduce that $\tilde{S}_{\rm crit} > 0$ for any $h \geq h_{\rm crit}$, which entails $\omega < 1/3$, in this region, and therefore the maximum value of ω is bounded, $\omega_{\rm max} < 1/3$. Due to the fact that $\omega_{\rm max}$ is the maximum value we have

$$\omega < 1/3 \tag{74}$$

for any h from the beginning of inflation until u it vanishes. This region certainly includes the end of inflation $h_{\rm end}$ and this puts an upper bound on the value of $\omega_{\rm end} \equiv \omega(h_{\rm end})$ at end of inflation; i.e.,

$$\omega_{\rm end} < 1/3. \tag{75}$$

Note that this is the analog of (58) for the minimally coupled models studied earlier. The bound (74) yields again the bound of (61), $c_s^2 > 2/3$, which results to (62), $\rho_{\rm end} < 1/4\alpha$. Therefore the bound (64) on the instantaneous temperature holds in the Higgs case as well.

For sufficiently large α, as in the case $\xi = 0$, the bound $\omega_{\rm end} \simeq 1/3$ is saturated. Then $\rho_{\rm end} = 1/4\alpha$ and the upper bound on $T_{\rm ins}$ of Eq. (64) is reached. With the aid of end of inflation relation (46) we get in a straightforward manner $RU_{\rm eff} = 5/12$, at end of inflation, or using the form of the potential as given in Eq. (15), $R_{\rm end} = 8\alpha/3$. This relation can be solved for $h_{\rm end}$, to derive the value of $h_{\rm end}$, when the upper bound on $T_{\rm ins}$ is reached. The solution is

$$(\sqrt{3c/5} - \xi)h_{\rm end}^2 = 1. \tag{76}$$

Note that this holds for sufficiently large α. We have verified that Eq. (76) indeed reproduces very accurately the numerical results for $h_{\rm end}$, for values $\alpha > \alpha_{\rm crit}$, with $\alpha_{\rm crit}$ given by where the coefficient of $h_{\rm end}^2$ on the left-hand side of (76) vanishes. This results to a critical value $\alpha_{\rm crit} = \frac{5}{3}(\frac{\xi^2}{\lambda})$. A last comment concerns the value of $\xi h_{\rm end}^2$ which turns out to be much smaller than unity in the regime $\alpha \gg \alpha_{\rm crit}$. In this case $g(h_{\rm end}) \simeq 1$ and hence predictions are expected to be same as with the $\xi = 0$ case. Anticipating the fact that the Higgs model can be in agreement with cosmological observations, as we shall discuss in the sequel, this by no means should lead us to the wrong conclusion that the simple quartic potential, $\xi = 0$, seen as the limiting case of the Higgs model, when $\xi h_{\rm end}^2 \ll 1$, can lead to successful inflation, In fact, $\xi h_{\rm end}^2 = (\sqrt{\alpha/\alpha_{\rm crit}} - 1)^{-1}$, and one needs $\alpha \geq 10^4\alpha_{\rm crit}$, or so, to obtain indeed small values $\xi h_{\rm end}^2 \leq 10^{-2}$. Such values for α outstrip the lower observational bound on n_s, as shown in Figs. 8 and 9, in which some representative outputs are displayed, and therefore are not acceptable. This is in perfect consistency with the statement made towards the end of previous sub-section that the simple quartic potential, $\xi = 0$ case, is in tension with n_s, predicting too low values for the spectral index.

Predictions of the Higgs model when the parameter ξ is small, $\xi = 0.1$, are shown at the top of Fig. 8. Denoting the quartic coupling by $\lambda = m^2$, the cases shown correspond to the lowest, $m = 2.85 \times 10^{-6}$, and largest, $m = 3.05 \times 10^{-6}$ allowed, when all observational data are observed and reheating is instantaneous. At the bottom of the same figure the case $\xi = 1.0$ is displayed. In this case the minimum and maximum allowed m values are $m = 9.10 \times 10^{-6}$ and $m = 9.70 \times 10^{-6}$, respectively.

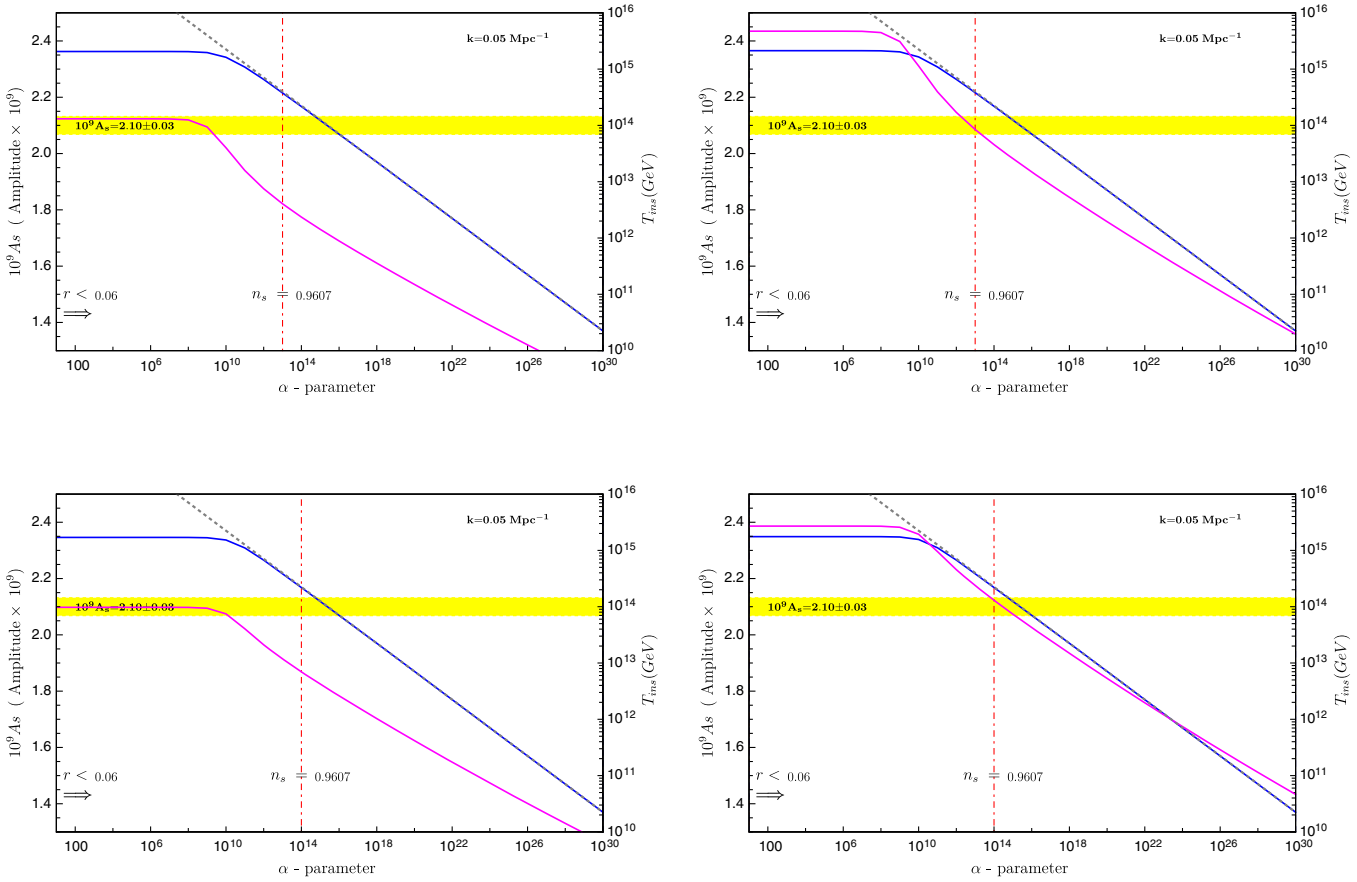

FIG. 8. As in Fig. 5, we display the bound set on the instantaneous reheating temperature, and other observables, for the Higgs model, $V(h) = \lambda h^4/4$. We have set $\lambda = m^2$ and the figures on top correspond to $\xi = 0.1$. For the top left pane $m = 2.85 \times 10^{-6}$ and for the right $m = 3.05 \times 10^{-6}$. These are the lowest and highest allowed m values when $\xi = 0.1$. The figures at the bottom correspond to $\xi = 1.0$. For the bottom left pane $m = 9.10 \times 10^{-6}$ and for the right $m = 9.70 \times 10^{-6}$. These are the lowest and highest allowed when $\xi = 1.0$. Note that in all cases displayed the bound for r has been moved to the far left so that all the α region is consistent with the bound $r < 0.06$ set on the tensor to scalar ratio.

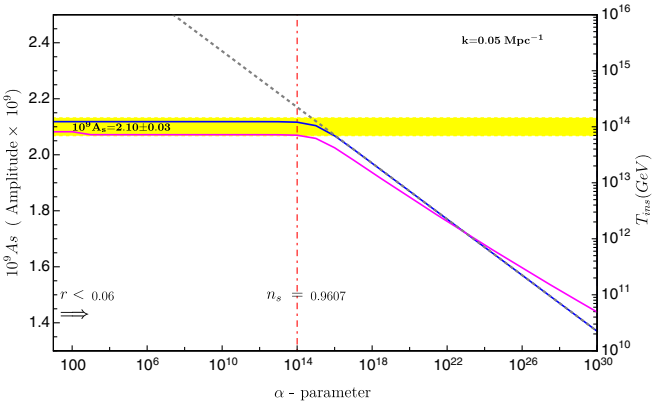

FIG. 9. As in Fig. 8, we display the bound set on the instantaneous reheating temperature, and other observables, for the Higgs model, for a large value $\xi = 10^5$. The case displayed corresponds to $m = 3.05 \times 10^{-3}$ which is the lowest allowed by all data for this value of ξ. A slight increase of m will move the A_s predictions off experimental bounds. Note that in this case the allowed region belongs to the slow-roll regime.

Given ξ, the min/max values of m and the ranges for the parameter α are shown in Table I. The corresponding ranges for the instantaneous temperature and the cosmological observables A_s, n_s, r, and the number of e-folds N_*, are also shown corresponding to a pivot scale $k^* = 0.05$ Mpc^{-1}. In all cases the value of r is small enough to satisfy the more stringent bound $r < 0.036$ put by BICEP/Keck observations [87]. For the maximum allowed value of m, the spectral index n_s is close to its lowest value, allowed by cosmological observations, while α gets its largest value. At the same time, the instantaneous reheating temperature gets its lowest value. These α values are in the regime where the quartic in the velocity terms contribute substantially and slow-roll approximation is not applicable. Thus, we need to go beyond slow-roll to derive these predictions, which has been done numerically. The lowest m values allow for a broad range $\alpha \lesssim 10^9$ and instantaneous temperature is larger. In this case, the inflationary dynamics can be successfully described by the slow-roll mechanism. The constancy of A_s for the lowest

TABLE I. Predictions of the Higgs model, for $\xi = 0.1$ and $\xi = 1.0$, when m gets its minimum and maximum allowed value allowed by all data, when reheating is instantaneous. The quartic coupling is $\lambda = m^2$. These are actually the cases displayed in Fig. 8. For the lowest m values allowed, a broad range of α is allowed, which is shrunk when m gets its maximum value. The corresponding ranges for the instantaneous temperature and the cosmological observables A_s, n_s, r, as well as the number of e-folds N_*, are also shown corresponding to a pivot scale $k^* = 0.05$ Mpc^{-1}.

Higgs model (pivot scale $k^* = 0.05$ Mpc^{-1})		
Value of $\xi = 0.1$		
min/max value of m :	$m = 2.85 \times 10^{-6}$	$m = 3.05 \times 10^{-6}$
α	10–10^9	$\simeq 10^{13}$
$T_{\rm ins}$	2.05×10^{15}–1.97×10^{15}	3.82×10^{14}
$10^9 A_s$	2.12–2.07	2.08
n_s	0.9638–0.9636	0.9609
r	0.006–0.004	$\sim 10^{-6}$
N_*	56.11–55.86	53.31
Value of $\xi = 1.0$		
min/max value of m :	$m = 9.10 \times 10^{-6}$	$m = 9.70 \times 10^{-6}$
α	10–10^{10}	$\simeq 10^{14}$
$T_{\rm ins}$	1.70×10^{15}–1.53×10^{15}	2.21×10^{14}
$10^9 A_s$	2.10–2.07	2.12
n_s	0.9632–0.9630	0.9610
r	0.0007–0.0004	$\sim 10^{-7}$
N_*	55.17–54.98	52.71

allowed m values actually follows from slow-roll. Using slow-roll approximation A_s is found to depend on the ratio c/α, that is on the parameter m alone and not on α. Note that for the lowest m case the tensor to scalar ratio is of the order of $r \sim 10^{-3}$, much larger, by almost 3 orders of magnitude, from the largest m case. These values will be therefore within reach by future missions aiming to probe small values of r as small as $r \sim 10^{-3}$, or so, [189,190].

One observes that the instantaneous temperature indeed touches the bound (64) for sufficiently large values of α, larger than some critical value $\alpha_{\rm crit}$ that indeed coincides with the one estimated previously, after Eq. (76), for each of the cases considered. Actually, $\alpha_{\rm crit}$ separates the two regimes. The slow-roll and the region of α for which the contribution of the quartic in the velocity terms is important in determining the end of inflation parameters. For low $\alpha < \alpha_{\rm crit}$ the instantaneous temperature stays well below the bound (64) and is rather insensitive to changes with α, for fixed values of ξ, m. This region belongs to the slow-roll regime and all data, including $T_{\rm ins}$, can be derived accurately enough employing the well-known methodology based on the slow-roll functions. For high $\alpha > \alpha_{\rm crit}$ slow-roll is not a valid approximation as we approach the end of inflation, and one should rely on a numerical treatment.

Lastly, in Fig. 9, we display the bound set on the instantaneous reheating temperature, and other observables, for the Higgs model, for a large value $\xi = 10^5$. The case displayed corresponds to $m = 3.05 \times 10^{-3}$ which is the lowest allowed by all data for this ξ. This is actually fine-tuned since by slightly increasing the value of m will move the A_s predictions off its experimental bounds. Note that this is a case where the entire allowed region falls within the slow-roll regime.

Concluding this section, we state that for the Higgs model, as for the quadratic potential, $V \sim h^2$ discussed in previous sections, and under the same conditions, the bounds derived when reheat is instantaneous, hold for lower temperatures, as well. In fact, for given ξ the range of the quartic coupling λ, which we derived assuming instantaneous reheating, hold true for lower temperatures, as well. The situation concerning bounds on the reheat temperature $T_{\rm reh}$, and on the parameter α, are similar to those of the minimally coupled model studied in the previous section, and thus need not be discussed in detail. However, there is an important difference, regarding the bound $r < 0.06$ which is much weaker in the nonminimal Higgs case ($\xi \neq 0$), allowing for much lower values of α, as low as $\alpha \simeq 10$, or even lower. Recall that in the case of the quadratic potential $V \sim h^2$, discussed in previous sections, α cannot be lower than about 10^8, due mainly to the aforementioned bound on the tensor to scalar ratio.

C. Summary of results—Discussion

The main results reached, for the models studied in this work, are summarized in the following.

For the Model I we have found that the allowed values for the mass parameter m lie within rather tight limits

$$6.2 \times 10^{-6} \lesssim m \lesssim 6.8 \times 10^{-6}, \tag{77}$$

while the range of acceptable α is

$$10^8 \lesssim \alpha \lesssim 10^{14}. \tag{78}$$

Values of $\alpha < 10^7$ are not allowed, violating the bound set on r, and higher values $\alpha > 10^{14}$ are incompatible with $n_s > 0.9607$. We remark that within the range (78), a critical value exists, $\alpha_{\rm crit} \simeq 10^{10}$, and for values of α beyond that the contribution of the quartic in the velocity terms are important in the determination of the end of inflation parameters. This is beyond the slow-roll regime. For such values of α the speed of sound approaches $c_s^2 \simeq 2/3$, its lowest mathematical bound in this kind of theories, and the upper bound set on the instantaneous temperature is saturated.

For any given m, within the range (77), there exists a range of α values, within (78), which are compatible with cosmological data. Assuming instantaneous reheating, and

when m gets its lowest value, in range (77), only values $\alpha \simeq 10^8$ are allowed. In this case we have the largest possible instantaneous temperature $T_{\rm ins} = 2.30 \times 10^{15}\,{\rm GeV}$. For this case $r \simeq 0.05$, that is close to its upper bound, and the spectral index is $n_s \simeq 0.9648$, that is it approaches its highest observational value. On the other hand, when m receives its largest value, within the range (77), the allowed α are near the upper limit of (78), $\alpha \simeq 10^{14}$. In this case we have the lowest possible instantaneous temperature $T_{\rm ins} \simeq 2.23 \times 10^{14}$ GeV while the value of r is very tiny $r \simeq 3 \times 10^{-8}$, and $n_s \simeq 0.9610$, that is close to its lowest observational bound.

Concerning the value of the tensor to scalar ratio r, this model is known to be in tension with r, predicting unacceptably large values in metric formulation. However the situation is rescued in the Palatini formulation thanks to the appearance of $\alpha\mathcal{R}^2$ terms in the action.

For the Higgs model, an additional parameter ξ exists, which controls the nonminimal coupling of inflaton to gravity. Given the parameter ξ, bounds are set on the quartic Higgs coupling λ, defined in (69), in the same way as for the Model I. For the benchmark values $\xi = 0.1$, 1.0 and $\xi = 10^5$, considered in this work, the allowed ranges for the parameter m, where $\lambda = m^2$, are as follows:

$$\begin{aligned} &\xi = 0.1\colon\ 2.85 \times 10^{-6} \lesssim m \lesssim 3.05 \times 10^{-6}, \\ &\xi = 1.0\colon\ 9.10 \times 10^{-6} \lesssim m \lesssim 9.70 \times 10^{-6}, \\ &\xi = 10^5\colon\ \simeq 3.05 \times 10^{-3}, \end{aligned} \tag{79}$$

while the range of acceptable α is

$$\alpha \lesssim 10^{14}. \tag{80}$$

Values of $\alpha > 10^{14}$ are incompatible with $n_s > 0.9607$. Note that there is no lower bound on α arising from $r < 0.06$, that is the r-bound weakens in the Higgs case. For the case of Higgs, a critical value exists, as well, given by $\alpha_{\rm crit} = \frac{5}{3}(\frac{\xi}{m})^2$, and for values of α larger than $\alpha_{\rm crit}$ the contribution of the quartic in the velocity terms are important, as in the case of Model I. In fact, for $\alpha > \alpha_{\rm crit}$ the speed of sound approaches $c_s^2 \simeq 2/3$, and the upper bound set on the instantaneous temperature is saturated. Note, however, that $\alpha_{\rm crit}$ exceeds the upper limit (80) for the case $\xi = 10^5$. This means that the contribution of the quartic in the velocity terms are negligible for values of α that are of physics interest to us, for this value of ξ.

For any m within (79), ranges of α values exist that are compatible with the cosmological data. For $\xi = 0.1$, the range of allowed α is $10 - 10^9$, when m gets its lowest value $m = 2.85 \times 10^{-6}$, with ranges of instantaneous temperature $T_{\rm ins} = 2.05 \times 10^{15} - 1.97 \times 10^{14}$ GeV. The value $T_{\rm ins} = 2.05 \times 10^{15}$ GeV is the largest possible. The tensor to scalar ratio r is in the range $r \simeq 0.006 - 0.004$, the highest values obtained in the Higgs model, while $n_s \simeq 0.9638 - 0.9636$. For the largest value $m = 3.05 \times 10^{-6}$ we can only have $\alpha \simeq 10^{13}$ and in this case $T_{\rm ins} = 3.82 \times 10^{14}$ GeV, while $r \simeq 8.0 \times 10^{-7}$, which is pretty small, and $n_s \simeq 0.9609$.

Passing to $\xi = 1.0$ case, for the smallest m, $m = 9.10 \times 10^{-6}$, the allowed range of α is $10 - 10^{10}$ with $T_{\rm ins} = 1.70 \times 10^{15} - 1.53 \times 10^{15}$ GeV and values of r in the range $r \simeq 7.0 \times 10^{-4} - 4.0 \times 10^{-4}$. As for the spectar index $n_s \simeq 0.9632 - 0.9630$. For the largest allowed m, $m = 9.70 \times 10^{-6}$ the α parameter is around $\alpha \simeq 10^{14}$, and in this case $T_{\rm ins} = 2.21 \times 10^{14}$ GeV, while r is very low $r \simeq 8.0 \times 10^{-8}$, and $n_s \simeq 0.9610$

Finally for the case $\xi = 10^5$, m is almost fine tuned to $m \simeq 3.05 \times 10^{-3}$. The allowed α values span the region $\alpha \simeq 10 - 10^{14}$, with $T_{\rm ins} = 1.23 \times 10^{14} - 1.21 \times 10^{13}$ GeV, while r is extremely low $r \simeq 7.5 \times 10^{-9}$ and $n_s \simeq 0.9608$.

Before leaving this section, we shall present a brief account of the metric and Palatini formulations of gravity. In Palatini gravity the affine connection Γ is an independent variable and it is through the equations of motion that is connected to the metric $g_{\mu\nu}$. In the absence of higher-R terms in the action, and if additional scalars are present, that are minimally coupled to gravity the affinity Γ becomes the well-known Levi-Civita connection $\Gamma = \Gamma(g)$ (Christoffel symbols). In this case the two theories yield identical results. However when nonminimal couplings exist and/or higher in the curvature R terms are present the two theories differ.

In the present work we have considered $\mathcal{R}^2$ terms coupled to Palatini gravity as $\alpha\mathcal{R}^2$ with α a constant. In the framework of metric gravity this theory describes, besides gravitons, the dynamics of a scalar propagating degree of freedom, the scalaron with mass $\sim 1/\sqrt{\alpha}$. This is best seen in the Einstein frame where the scalaron appears as a scalar field, which plays the role of the inflaton, moving under the influence of the Starobinsky potential, which is predicted and not put in by hand. In the framework of Palatini gravity the inclusion of $\alpha\mathcal{R}^2$ terms differs from the Starobinsky case of metric formulation. There are no extra propagating degrees of freedom and the would-be inflaton, as well as its potential, have to be introduced explicitly. Note that the inclusion of additional scalars in the metric formulation, when $\alpha\mathcal{R}^2$ is present, leads to multifield inflation in the Einstein frame.

The inclusion of $\alpha\mathcal{R}^2$ in Palatini action has two important consequences. It flattens the scalar potential in the Einstein frame, even for a steep original potential $V(h)$, and a plateau is created, for large field values, which can sustain inflation. Besides, it induces quartic terms in the velocity which affect the inflaton evolution towards the end of inflation for large values of the coupling α, larger than some critical value. Both of these features are absent in the limit of α tending to zero, that is for sufficiently small couplings, and thus are expected to play little role in the small α

regime. Note that the absence of $\alpha\mathcal{R}^2$ terms does not imply that metric and Palatini formulations lead to equivalent theories. In fact, if nonminimal couplings are present, as in the Higgs case, for instance, the two formalisms lead to different actions in the Einstein frame and thus to different inflationary models.

On the phenomenological side, the inclusion of $\alpha\mathcal{R}^2$ terms is well known to lower the value of r for any inflationary model [31–33]. The quadratic potential $\sim h^2$ belongs to this class which is given unacceptable values for r in metric formulation but it survives in the Palatini gravity, as we have seen. Also in the Higgs case the values of r are systematically lower than the Higgs inflation in metric formulation. Also the values of the non-minimal coupling ξ can take much lower values in the Palatini formulation.

VI. CONCLUSIONS

We have studied models of $\mathcal{R}^2$ inflation in the framework of Palatini gravity, where the coupling of the $\mathcal{R}^2$ to gravity is of the form $\sim\alpha\mathcal{R}^2$, with α is constant. The appearance of terms which are quartic in the velocity of inflaton is unavoidable in these theories. These play a little role, as being very small, during the first horizon crossing, however, they may play an important role in determining the end of inflation dynamics, and, in particular, the instantaneous reheating temperature, when the scale α is large. We have found that there is some critical value of α below which the mechanism of inflation follows slow-roll during the whole inflation era. However, above this, the inflationary evolution deviates from slow-roll, as the inflaton approaches the end of inflation, defined by where the acceleration $\ddot{a}$ of the cosmic scale factor vanishes. In this case the determination of the end of inflaton is inaccurate when slow-roll is employed. In a class of popular models, the speed of sound is bounded by $c_s^2 \geq 2/3$, putting upper bounds on the instantaneous reheating temperature $T_{\rm ins}$, given by $T_{\rm ins} \leq 0.290 m_{\rm Planck}/\alpha^{1/4}$. These bounds are saturated for large values of α.

Assuming instantaneous reheating, we have derived bounds on the parameters of the models studied in this work, arising from the amplitude of the scalar power spectrum A_s, the spectral index n_s, and the tensor to scalar ratio r. The instantaneous reheating temperature cannot be arbitrarily small since the scale α is bounded from above by observations, imposing in turn lower bounds on the inflationary scale. For the models considered it is found that α cannot exceed $\alpha \simeq 10^{14}$, arising from n_s data, which for the largest α touches its lowest observational limit.

When reheating is not instantaneous, predictions depend on the value of the effective equation of state parameter w. However, the constraints on the coupling of the scalar potential remain the same. For reasonable values of w, in the range $w \simeq 0.0$–0.25, the allowed values of α lie in a certain range, constraining the reheat temperature $T_{\rm reh}$ to be within a range dictated by the value of α taken. When the coupling of the scalar potential gets its minimum allowed value we obtain the highest possible temperature. This is independent of the value of w taken. In fact, this is the instantaneous temperature corresponding to the smallest allowed value of α, which receives its lowest possible value allowed by all data in this case. Then temperatures as large as $\sim 10^{15}$ GeV can be reached, in principle, for the models studied in this work. Low values can be also obtained, as low as $\simeq$MeV, when the equation of state parameter is $w \simeq 0.25$, or higher. The acceptable values of α in this case are larger than $\sim 10^{10}$, within the regime where slow-roll is not applicable. In this case, we need to go beyond slow-roll for a reliable cosmological study.

ACKNOWLEDGMENTS

A. B. L. wishes to thank I. D. Gialamas for discussions at the initial stages of this work. He also thanks V. C. Spanos and K. Tamvakis for illuminating discussions.

[1] T. P. Sotiriou, $f(R)$ gravity and scalar-tensor theory, Classical Quantum Gravity **23**, 5117 (2006).
[2] T. P. Sotiriou and S. Liberati, Metric-affine $f(R)$ theories of gravity, Ann. Phys. (Amsterdam) **322**, 935 (2007).
[3] T. P. Sotiriou and V. Faraoni, $f(R)$ theories of gravity, Rev. Mod. Phys. **82**, 451 (2010).
[4] M. Borunda, B. Janssen, and M. Bastero-Gil, Palatini versus metric formulation in higher curvature gravity, J. Cosmol. Astropart. Phys. 11 (2008) 008.
[5] A. De Felice and S. Tsujikawa, $f(R)$ theories, Living Rev. Relativity **13**, 3 (2010).
[6] G. J. Olmo, Palatini approach to modified gravity: $f(R)$ theories and beyond, Int. J. Mod. Phys. D **20**, 413 (2011).
[7] S. Capozziello and M. De Laurentis, Extended theories of gravity, Phys. Rep. **509**, 167 (2011).
[8] T. Clifton, P. G. Ferreira, A. Padilla, and C. Skordis, Modified gravity and cosmology, Phys. Rep. **513**, 1 (2012).
[9] S. Nojiri, S. D. Odintsov, and V. K. Oikonomou, Modified gravity theories on a nutshell: Inflation, bounce and late-time evolution, Phys. Rep. **692**, 1 (2017).

[10] A. A. Starobinsky, A new type of isotropic cosmological models without singularity, Phys. Lett. **91B**, 99 (1980); Adv. Ser. Astrophys. Cosmol. **3**, 130 (1987).
[11] V. F. Mukhanov and G. V. Chibisov, Quantum fluctuations and a nonsingular universe, Pis'ma Zh. Eksp. Teor. Fiz. **33**, 549 (1981) [JETP Lett. **33**, 532 (1981)].
[12] A. A. Starobinsky, The perturbation spectrum evolving from a nonsingular initially de-Sitter cosmology and the microwave background anisotropy, Sov. Astron. Lett. **9**, 302 (1983).
[13] F. Bauer and D. A. Demir, Inflation with non-minimal coupling: Metric versus Palatini formulations, Phys. Lett. B **665**, 222 (2008).
[14] T. Koivisto and H. Kurki-Suonio, Cosmological perturbations in the Palatini formulation of modified gravity, Classical Quantum Gravity **23**, 2355 (2006).
[15] N. Tamanini and C. R. Contaldi, Inflationary perturbations in Palatini generalised gravity, Phys. Rev. D **83**, 044018 (2011).
[16] F. Bauer and D. A. Demir, Higgs-Palatini inflation and unitarity, Phys. Lett. B **698**, 425 (2011).
[17] K. Enqvist, T. Koivisto, and G. Rigopoulos, Non-metric chaotic inflation, J. Cosmol. Astropart. Phys. 05 (2012) 023.
[18] A. Borowiec, M. Kamionka, A. Kurek, and M. Szydlowski, Cosmic acceleration from modified gravity with Palatini formalism, J. Cosmol. Astropart. Phys. 02 (2012) 027.
[19] A. Stachowski, M. Szydlowski, and A. Borowiec, Starobinsky cosmological model in Palatini formalism, Eur. Phys. J. C **77**, 406 (2017).
[20] C. Fu, P. Wu, and H. Yu, Inflationary dynamics and preheating of the nonminimally coupled inflaton field in the metric and Palatini formalisms, Phys. Rev. D **96**, 103542 (2017).
[21] S. Rasanen and P. Wahlman, Higgs inflation with loop corrections in the Palatini formulation, J. Cosmol. Astropart. Phys. 11 (2017) 047.
[22] T. Tenkanen, Resurrecting quadratic inflation with a non-minimal coupling to gravity, J. Cosmol. Astropart. Phys. 12 (2017) 001.
[23] A. Racioppi, Coleman-Weinberg linear inflation: Metric vs Palatini formulation, J. Cosmol. Astropart. Phys. 12 (2017) 041.
[24] T. Markkanen, T. Tenkanen, V. Vaskonen, and H. Veermäe, Quantum corrections to quartic inflation with a non-minimal coupling: Metric vs Palatini, J. Cosmol. Astropart. Phys. 03 (2018) 029.
[25] L. Järv, A. Racioppi, and T. Tenkanen, Palatini side of inflationary attractors, Phys. Rev. D **97**, 083513 (2018).
[26] S. Rasanen, Higgs inflation in the Palatini formulation with kinetic terms for the metric, Open J. Astrophys. **2**, 1 (2019).
[27] A. Racioppi, New universal attractor in nonminimally coupled gravity: Linear inflation, Phys. Rev. D **97**, 123514 (2018).
[28] P. Carrilho, D. Mulryne, J. Ronayne, and T. Tenkanen, Attractor behaviour in multifield inflation, J. Cosmol. Astropart. Phys. 06 (2018) 032.
[29] V. M. Enckell, K. Enqvist, S. Rasanen, and E. Tomberg, Higgs inflation at the hilltop, J. Cosmol. Astropart. Phys. 06 (2018) 005.
[30] F. Bombacigno and G. Montani, Big bounce cosmology for Palatini R^2 gravity with a Nieh-Yan term, Eur. Phys. J. C **79**, 405 (2019).
[31] V. M. Enckell, K. Enqvist, S. Rasanen, and L. P. Wahlman, Inflation with R^2 term in the Palatini formalism, J. Cosmol. Astropart. Phys. 02 (2019) 022.
[32] I. Antoniadis, A. Karam, A. Lykkas, and K. Tamvakis, Palatini inflation in models with an R^2 term, J. Cosmol. Astropart. Phys. 11 (2018) 028.
[33] I. Antoniadis, A. Karam, A. Lykkas, T. Pappas, and K. Tamvakis, Rescuing quartic and natural inflation in the Palatini formalism, J. Cosmol. Astropart. Phys. 03 (2019) 005.
[34] S. Rasanen and E. Tomberg, Planck scale black hole dark matter from Higgs inflation, J. Cosmol. Astropart. Phys. 01 (2019) 038.
[35] J. P. B. Almeida, N. Bernal, J. Rubio, and T. Tenkanen, Hidden inflaton dark matter, J. Cosmol. Astropart. Phys. 03 (2019) 012.
[36] T. Takahashi and T. Tenkanen, Towards distinguishing variants of non-minimal inflation, J. Cosmol. Astropart. Phys. 04 (2019) 035.
[37] K. Kannike, A. Kubarski, L. Marzola, and A. Racioppi, A minimal model of inflation and dark radiation, Phys. Lett. B **792**, 74 (2019).
[38] T. Tenkanen, Minimal Higgs inflation with an R^2 term in Palatini gravity, Phys. Rev. D **99**, 063528 (2019).
[39] K. Shimada, K. Aoki, and K. i. Maeda, Metric-affine gravity and inflation, Phys. Rev. D **99**, 104020 (2019).
[40] J. Wu, G. Li, T. Harko, and S. D. Liang, Palatini formulation of $f(R,T)$ gravity theory, and its cosmological implications, Eur. Phys. J. C **78**, 430 (2018).
[41] A. Kozak and A. Borowiec, Palatini frames in scalar tensor theories of gravity, Eur. Phys. J. C **79**, 335 (2019).
[42] R. Jinno, K. Kaneta, K. y. Oda, and S. C. Park, Hill-climbing inflation in metric and Palatini formulations, Phys. Lett. B **791**, 396 (2019).
[43] A. Edery and Y. Nakayama, Palatini formulation of pure R^2 gravity yields Einstein gravity with no massless scalar, Phys. Rev. D **99**, 124018 (2019).
[44] J. Rubio and E. S. Tomberg, Preheating in Palatini Higgs inflation, J. Cosmol. Astropart. Phys. 04 (2019) 021.
[45] R. Jinno, M. Kubota, K. y. Oda, and S. C. Park, Higgs inflation in metric and Palatini formalisms: Required suppression of higher dimensional operators, J. Cosmol. Astropart. Phys. 03 (2020) 063.
[46] M. Giovannini, Post-inflationary phases stiffer than radiation and Palatini formulation, Classical Quantum Gravity **36**, 235017 (2019).
[47] T. Tenkanen and L. Visinelli, Axion dark matter from Higgs inflation with an intermediate H_*, J. Cosmol. Astropart. Phys. 08 (2019) 033.
[48] N. Bostan, Non-minimally coupled quartic inflation with Coleman-Weinberg one-loop corrections in the Palatini formulation, Phys. Lett. B **811**, 135954 (2020).
[49] N. Bostan, Quadratic, Higgs and hilltop potentials in the Palatini gravity, Commun. Theor. Phys. **72**, 085401 (2020).
[50] T. Tenkanen, Trans-Planckian censorship, inflation, and dark matter, Phys. Rev. D **101**, 063517 (2020).

[51] I. D. Gialamas and A. B. Lahanas, Reheating in R^2 Palatini inflationary models, Phys. Rev. D **101**, 084007 (2020).

[52] A. Racioppi, Non-minimal (Self-)running inflation: Metric vs Palatini formulation, J. High Energy Phys. 21 (2020) 011.

[53] T. Tenkanen, Tracing the high energy theory of gravity: An introduction to Palatini inflation, Gen. Relativ. Gravit. **52**, 33 (2020).

[54] A. Lloyd-Stubbs and J. McDonald, Sub-Planckian ϕ^2 inflation in the Palatini formulation of gravity with an R^2 term, Phys. Rev. D **101**, 123515 (2020).

[55] T. Tenkanen and E. Tomberg, Initial conditions for plateau inflation: A case study, J. Cosmol. Astropart. Phys. 04 (2020) 050.

[56] N. Das and S. Panda, Inflation and reheating in $f(R, h)$ theory formulated in the Palatini formalism, J. Cosmol. Astropart. Phys. 05 (2021) 019.

[57] J. McDonald, Does Palatini Higgs inflation conserve unitarity?, J. Cosmol. Astropart. Phys. 04 (2021) 069.

[58] M. Shaposhnikov, A. Shkerin, and S. Zell, Quantum effects in Palatini Higgs inflation, J. Cosmol. Astropart. Phys. 07 (2020) 064.

[59] S. Bekov, K. Myrzakulov, R. Myrzakulov, and D. S. C. Gómez, General slow-roll inflation in $f(R)$ gravity under the Palatini approach, Symmetry **12**, 1958 (2020).

[60] V. M. Enckell, S. Nurmi, S. Räsänen, and E. Tomberg, Critical point Higgs inflation in the Palatini formulation, J. High Energy Phys. 04 (2021) 059.

[61] A. Lykkas and K. Tamvakis, Extended interactions in the Palatini-R^2 inflation, J. Cosmol. Astropart. Phys. 08 (2021) 043.

[62] L. Järv, A. Karam, A. Kozak, A. Lykkas, A. Racioppi, and M. Saal, Equivalence of inflationary models between the metric and Palatini formulation of scalar-tensor theories, Phys. Rev. D **102**, 044029 (2020).

[63] A. Karam, S. Karamitsos, and M. Saal, β-function reconstruction of Palatini inflationary attractors, J. Cosmol. Astropart. Phys. 10 (2021) 068.

[64] I. D. Gialamas, A. Karam, and A. Racioppi, Dynamically induced Planck scale and inflation in the Palatini formulation, J. Cosmol. Astropart. Phys. 11 (2020) 014.

[65] A. Karam, M. Raidal, and E. Tomberg, Gravitational dark matter production in Palatini preheating, J. Cosmol. Astropart. Phys. 03 (2021) 064.

[66] I. D. Gialamas, A. Karam, A. Lykkas, and T. D. Pappas, Palatini-Higgs inflation with nonminimal derivative coupling, Phys. Rev. D **102**, 063522 (2020).

[67] A. Karam, E. Tomberg, and H. Veermäe, Tachyonic preheating in Palatini R 2 inflation, J. Cosmol. Astropart. Phys. 06 (2021) 023.

[68] I. D. Gialamas, A. Karam, T. D. Pappas, and V. C. Spanos, Scale-invariant quadratic gravity and inflation in the Palatini formalism, Phys. Rev. D **104**, 023521 (2021).

[69] I. D. Gialamas, A. Karam, T. D. Pappas, A. Racioppi, and V. C. Spanos, Scale-invariance, dynamically induced Planck scale and inflation in the Palatini formulation, J. Phys. Conf. Ser. **2105**, 012005 (2021).

[70] J. Annala and S. Rasanen, Inflation with R ($\alpha\beta$) terms in the Palatini formulation, J. Cosmol. Astropart. Phys. 09 (2021) 032.

[71] A. Racioppi, J. Rajasalu, and K. Selke, Multiple point criticality principle and Coleman-Weinberg inflation, J. High Energy Phys. 06 (2022) 107.

[72] M. Giovannini, Palatini approach and large-scale magnetogenesis, J. Cosmol. Astropart. Phys. 11 (2021) 058.

[73] D. Y. Cheong, S. M. Lee, and S. C. Park, Reheating in models with non-minimal coupling in metric and Palatini formalisms, J. Cosmol. Astropart. Phys. 02 (2022) 029.

[74] Y. Mikura and Y. Tada, On UV-completion of Palatini-Higgs inflation, J. Cosmol. Astropart. Phys. 05 (2022) 035.

[75] C. Dioguardi, A. Racioppi, and E. Tomberg, Slow-roll inflation in Palatini $F(R)$ gravity, J. High Energy Phys. 06 (2022) 106.

[76] A. Ito, W. Khater, and S. Rasanen, Tree-level unitarity in Higgs inflation in the metric and the Palatini formulation, J. High Energy Phys. 06 (2022) 164.

[77] A. Racioppi and M. Vasar, On the number of e-folds in the Jordan and Einstein frames, Eur. Phys. J. Plus **137**, 637 (2022).

[78] C. Rigouzzo and S. Zell, Coupling metric-affine gravity to a Higgs-like scalar field, Phys. Rev. D **106**, 024015 (2022).

[79] K. Dimopoulos and S. Sánchez López, Quintessential inflation in Palatini $f(R)$ gravity, Phys. Rev. D **103**, 043533 (2021).

[80] K. Dimopoulos, A. Karam, S. Sánchez López, and E. Tomberg, Modelling quintessential inflation in Palatini-modified gravity, Galaxies **10**, 57 (2022).

[81] F. Dux, A. Florio, J. Klarić, A. Shkerin, and I. Timiryasov, Preheating in Palatini Higgs inflation on the lattice, J. Cosmol. Astropart. Phys. 09 (2022) 015.

[82] K. Dimopoulos, A. Karam, S. Sánchez López, and E. Tomberg, Palatini R^2 quintessential inflation, J. Cosmol. Astropart. Phys. 10 (2022) 076.

[83] M. He, Y. Mikura, and Y. Tada, Hybrid metric-Palatini Higgs inflation, arXiv:2209.11051.

[84] N. Aghanim *et al.* (Planck Collaboration), Planck 2018 results. VI. Cosmological parameters, Astron. Astrophys. **641**, A6 (2020); **652**, C4 (2021).

[85] Y. Akrami *et al.* (Planck Collaboration), Planck 2018 results. X. Constraints on inflation, Astron. Astrophys. **641**, A10 (2020).

[86] P. A. R. Ade *et al.* (BICEP2 and Keck Array Collaborations), BICEP2 / Keck Array x: Constraints on Primordial Gravitational Waves Using Planck, WMAP, and New BICEP2/Keck Observations Through the 2015 Season, Phys. Rev. Lett. **121**, 221301 (2018).

[87] P. A. R. Ade *et al.* (BICEP and Keck Collaborations), Improved Constraints on Primordial Gravitational Waves using Planck, WMAP, and BICEP/Keck Observations through the 2018 Observing Season, Phys. Rev. Lett. **127**, 151301 (2021).

[88] M. Gerbino, K. Freese, S. Vagnozzi, M. Lattanzi, O. Mena, E. Giusarma, and S. Ho, Impact of neutrino properties on the estimation of inflationary parameters from current and future observations, Phys. Rev. D **95**, 043512 (2017).

[89] C. Armendariz-Picon, T. Damour, and V. F. Mukhanov, k—inflation, Phys. Lett. B **458**, 209 (1999).

[90] J. Garriga and V. F. Mukhanov, Perturbations in k-inflation, Phys. Lett. B **458**, 219 (1999).

[91] L. Lorenz, J. Martin, and C. Ringeval, Constraints on kinetically modified inflation from WMAP5, Phys. Rev. D **78**, 063543 (2008).
[92] S. Li and A. R. Liddle, Observational constraints on K-inflation models, J. Cosmol. Astropart. Phys. 10 (2012) 011.
[93] S. Nojiri, S. D. Odintsov, and V. K. Oikonomou, k-essence $f(R)$ gravity inflation, Nucl. Phys. **B941**, 11 (2019).
[94] S. D. Odintsov and V. K. Oikonomou, Constant-roll k-inflation dynamics, Classical Quantum Gravity **37**, 025003 (2020).
[95] Y. Mikura, Y. Tada, and S. Yokoyama, Minimal k-inflation in light of the conformal metric-affine geometry, Phys. Rev. D **103**, L101303 (2021).
[96] P. Pareek and A. Nautiyal, Reheating constraints on k-inflation, Phys. Rev. D **104**, 083526 (2021).
[97] S. D. Odintsov, V. K. Oikonomou, and F. P. Fronimos, k-inflation-corrected Einstein-Gauss-Bonnet gravity with massless primordial gravitons, Nucl. Phys. **B963**, 115299 (2021).
[98] V. K. Oikonomou, Non-minimally coupled scalar k-inflation dynamics, Eur. Phys. J. Plus **136**, 155 (2021).
[99] A. R. Liddle, P. Parsons, and J. D. Barrow, Formalizing the slow roll approximation in inflation, Phys. Rev. D **50**, 7222 (1994).
[100] J. Ellis, M. A. G. Garcia, D. V. Nanopoulos, and K. A. Olive, Calculations of inflaton decays and reheating: With applications to no-scale inflation models, J. Cosmol. Astropart. Phys. 07 (2015) 050.
[101] L. Kofman, A. D. Linde, and A. A. Starobinsky, Reheating After Inflation, Phys. Rev. Lett. **73**, 3195 (1994).
[102] Y. Shtanov, J. H. Traschen, and R. H. Brandenberger, Universe reheating after inflation, Phys. Rev. D **51**, 5438 (1995).
[103] L. Kofman, A. D. Linde, and A. A. Starobinsky, Towards the theory of reheating after inflation, Phys. Rev. D **56**, 3258 (1997).
[104] D. J. H. Chung, E. W. Kolb, and A. Riotto, Production of massive particles during reheating, Phys. Rev. D **60**, 063504 (1999).
[105] M. Kawasaki, K. Kohri, and N. Sugiyama, Cosmological Constraints on Late Time Entropy Production, Phys. Rev. Lett. **82**, 4168 (1999).
[106] S. Davidson and S. Sarkar, Thermalization after inflation, J. High Energy Phys. 11 (2000) 012.
[107] G. F. Giudice, E. W. Kolb, and A. Riotto, Largest temperature of the radiation era and its cosmological implications, Phys. Rev. D **64**, 023508 (2001).
[108] J. Martin and C. Ringeval, First CMB constraints on the inflationary reheating temperature, Phys. Rev. D **82**, 023511 (2010).
[109] R. Allahverdi, R. Brandenberger, F. Y. Cyr-Racine, and A. Mazumdar, Reheating in inflationary cosmology: Theory and applications, Annu. Rev. Nucl. Part. Sci. **60**, 27 (2010).
[110] D. I. Podolsky, G. N. Felder, L. Kofman, and M. Peloso, Equation of state and beginning of thermalization after preheating, Phys. Rev. D **73**, 023501 (2006).
[111] P. Adshead, R. Easther, J. Pritchard, and A. Loeb, Inflation and the scale dependent spectral index: Prospects and strategies, J. Cosmol. Astropart. Phys. 02 (2011) 021.
[112] J. Mielczarek, Reheating temperature from the CMB, Phys. Rev. D **83**, 023502 (2011).
[113] R. Easther and H. V. Peiris, Bayesian analysis of inflation II: Model selection and constraints on reheating, Phys. Rev. D **85**, 103533 (2012).
[114] L. Dai, M. Kamionkowski, and J. Wang, Reheating Constraints to Inflationary Models, Phys. Rev. Lett. **113**, 041302 (2014).
[115] K. Harigaya and K. Mukaida, Thermalization after/during reheating, J. High Energy Phys. 05 (2014) 006.
[116] J. B. Munoz and M. Kamionkowski, Equation-of-state parameter for reheating, Phys. Rev. D **91**, 043521 (2015).
[117] J. L. Cook, E. Dimastrogiovanni, D. A. Easson, and L. M. Krauss, Reheating predictions in single field inflation, J. Cosmol. Astropart. Phys. 04 (2015) 047.
[118] J. O. Gong, S. Pi, and G. Leung, Probing reheating with primordial spectrum, J. Cosmol. Astropart. Phys. 05 (2015) 027.
[119] T. Rehagen and G. B. Gelmini, Low reheating temperatures in monomial and binomial inflationary potentials, J. Cosmol. Astropart. Phys. 06 (2015) 039.
[120] M. Drewes, What can the CMB tell about the microphysics of cosmic reheating?, J. Cosmol. Astropart. Phys. 03 (2016) 013.
[121] R. G. Cai, Z. K. Guo, and S. J. Wang, Reheating phase diagram for single-field slow-roll inflationary models, Phys. Rev. D **92**, 063506 (2015).
[122] R. C. de Freitas and S. V. B. Gonçalves, CMB constraints on reheating models with varying equation of state, arXiv:1509.08500.
[123] K. D. Lozanov and M. A. Amin, Equation of State and Duration to Radiation Domination after Inflation, Phys. Rev. Lett. **119**, 061301 (2017).
[124] K. D. Lozanov and M. A. Amin, Self-resonance after inflation: Oscillons, transients and radiation domination, Phys. Rev. D **97**, 023533 (2018).
[125] I. Dalianis, G. Koutsoumbas, K. Ntrekis, and E. Papantonopoulos, Reheating predictions in gravity theories with derivative coupling, J. Cosmol. Astropart. Phys. 02 (2017) 027.
[126] T. Hasegawa, N. Hiroshima, K. Kohri, R. S. L. Hansen, T. Tram, and S. Hannestad, MeV-scale reheating temperature and thermalization of oscillating neutrinos by radiative and hadronic decays of massive particles, J. Cosmol. Astropart. Phys. 12 (2019) 012.
[127] A. Di Marco, G. Pradisi, and P. Cabella, Inflationary scale, reheating scale, and pre-BBN cosmology with scalar fields, Phys. Rev. D **98**, 123511 (2018).
[128] M. He, R. Jinno, K. Kamada, S. C. Park, A. A. Starobinsky, and J. Yokoyama, On the violent preheating in the mixed Higgs-R^2 inflationary model, Phys. Lett. B **791**, 36 (2019).
[129] G. German, Model independent results for the inflationary epoch and the breaking of the degeneracy of models of inflation, J. Cosmol. Astropart. Phys. 11 (2020) 006.
[130] P. Saha, S. Anand, and L. Sriramkumar, Accounting for the time evolution of the equation of state parameter during reheating, Phys. Rev. D **102**, 103511 (2020).
[131] Y. Hamada, K. Kawana, and A. Scherlis, On preheating in Higgs inflation, J. Cosmol. Astropart. Phys. 03 (2021) 062.

[132] M. He, R. Jinno, K. Kamada, A. A. Starobinsky, and J. Yokoyama, Occurrence of tachyonic preheating in the mixed Higgs-R^2 model, J. Cosmol. Astropart. Phys. 01 (2021) 066.

[133] M. He, Perturbative reheating in the mixed Higgs-R^2 model, J. Cosmol. Astropart. Phys. 05 (2021) 021.

[134] A. Di Marco and G. Pradisi, Variable inflaton equation-of-state and reheating, Int. J. Mod. Phys. A **36**, 2150095 (2021).

[135] S. Kawai and N. Okada, Gravitino constraints on supergravity inflation, Phys. Rev. D **105**, L101302 (2022).

[136] A. R. Liddle and S. M. Leach, How long before the end of inflation were observable perturbations produced?, Phys. Rev. D **68**, 103503 (2003).

[137] S. Dodelson and L. Hui, A Horizon Ratio Bound for Inflationary Fluctuations, Phys. Rev. Lett. **91**, 131301 (2003).

[138] J. J. M. Carrasco, R. Kallosh, and A. Linde, α-attractors: Planck, LHC and dark energy, J. High Energy Phys. 10 (2015) 147.

[139] J. J. M. Carrasco, R. Kallosh, and A. Linde, Cosmological attractors and initial conditions for inflation, Phys. Rev. D **92**, 063519 (2015).

[140] A. A. Starobinsky, Spectrum of relict gravitational radiation and the early state of the universe, Pis'ma Zh. Eksp. Teor. Fiz. **30**, 719 (1979) [JETP Lett. **30**, 682 (1979)].

[141] V. F. Mukhanov, Gravitational instability of the universe filled with a scalar field, Pis'ma Zh. Eksp. Teor. Fiz. **41**, 402 (1985) [JETP Lett. **41**, 493 (1985)].

[142] V. F. Mukhanov, Zh. Eksp. Teor. Fiz. **94N7**, 1 (1988) [Sov. Phys. JETP **67**, 1297 (1988)].

[143] F. Lucchin and S. Matarrese, Power law inflation, Phys. Rev. D **32**, 1316 (1985).

[144] E. D. Stewart and D. H. Lyth, A more accurate analytic calculation of the spectrum of cosmological perturbations produced during inflation, Phys. Lett. B **302**, 171 (1993).

[145] J. O. Gong and E. D. Stewart, The density perturbation power spectrum to second order corrections in the slow roll expansion, Phys. Lett. B **510**, 1 (2001).

[146] D. J. Schwarz, C. A. Terrero-Escalante, and A. A. Garcia, Higher order corrections to primordial spectra from cosmological inflation, Phys. Lett. B **517**, 243 (2001).

[147] S. M. Leach, A. R. Liddle, J. Martin, and D. J. Schwarz, Cosmological parameter estimation and the inflationary cosmology, Phys. Rev. D **66**, 023515 (2002).

[148] S. Habib, K. Heitmann, G. Jungman, and C. Molina-Paris, The Inflationary Perturbation Spectrum, Phys. Rev. Lett. **89**, 281301 (2002).

[149] J. Martin and D. J. Schwarz, WKB approximation for inflationary cosmological perturbations, Phys. Rev. D **67**, 083512 (2003).

[150] S. Habib, A. Heinen, K. Heitmann, G. Jungman, and C. Molina-Paris, Characterizing inflationary perturbations: The uniform approximation, Phys. Rev. D **70**, 083507 (2004).

[151] H. Wei, R. G. Cai, and A. Wang, Second-order corrections to the power spectrum in the slow-roll expansion with a time-dependent sound speed, Phys. Lett. B **603**, 95 (2004).

[152] R. Casadio, F. Finelli, M. Luzzi, and G. Venturi, Improved WKB analysis of cosmological perturbations, Phys. Rev. D **71**, 043517 (2005).

[153] R. Casadio, F. Finelli, M. Luzzi, and G. Venturi, Higher order slow-roll predictions for inflation, Phys. Lett. B **625**, 1 (2005).

[154] W. H. Kinney and K. Tzirakis, Quantum modes in DBI inflation: Exact solutions and constraints from vacuum selection, Phys. Rev. D **77**, 103517 (2008).

[155] L. Lorenz, J. Martin, and C. Ringeval, K-inflationary power spectra in the uniform approximation, Phys. Rev. D **78**, 083513 (2008).

[156] N. Agarwal and R. Bean, Cosmological constraints on general, single field inflation, Phys. Rev. D **79**, 023503 (2009).

[157] J. Martin, C. Ringeval, and V. Vennin, K-inflationary power spectra at second order, J. Cosmol. Astropart. Phys. 06 (2013) 021.

[158] J. Beltran Jimenez, M. Musso, and C. Ringeval, Exact mapping between tensor and most general scalar power spectra, Phys. Rev. D **88**, 043524 (2013).

[159] A. L. Alinea, T. Kubota, and W. Naylor, Logarithmic divergences in the k-inflationary power spectra computed through the uniform approximation, J. Cosmol. Astropart. Phys. 02 (2016) 028.

[160] S. Pi, Y. l. Zhang, Q. G. Huang, and M. Sasaki, Scalaron from R^2-gravity as a heavy field, J. Cosmol. Astropart. Phys. 05 (2018) 042.

[161] F. L. Bezrukov and M. Shaposhnikov, The standard model Higgs boson as the inflaton, Phys. Lett. B **659**, 703 (2008).

[162] F. L. Bezrukov, A. Magnin, and M. Shaposhnikov, Standard model Higgs boson mass from inflation, Phys. Lett. B **675**, 88 (2009).

[163] J. L. F. Barbon and J. R. Espinosa, On the naturalness of Higgs inflation, Phys. Rev. D **79**, 081302 (2009).

[164] A. O. Barvinsky, A. Y. Kamenshchik, C. Kiefer, A. A. Starobinsky, and C. Steinwachs, Asymptotic freedom in inflationary cosmology with a non-minimally coupled Higgs field, J. Cosmol. Astropart. Phys. 12 (2009) 003.

[165] A. O. Barvinsky, A. Y. Kamenshchik, C. Kiefer, A. A. Starobinsky, and C. F. Steinwachs, Higgs boson, renormalization group, and naturalness in cosmology, Eur. Phys. J. C **72**, 2219 (2012).

[166] C. Germani and A. Kehagias, New Model of Inflation with Non-minimal Derivative Coupling of Standard Model Higgs Boson to Gravity, Phys. Rev. Lett. **105**, 011302 (2010).

[167] C. Germani and A. Kehagias, Cosmological Perturbations in the New Higgs Inflation, J. Cosmol. Astropart. Phys. 05 (2010) 019; 06 (2010) 01.

[168] R. N. Lerner and J. McDonald, A unitarity-conserving Higgs inflation model, Phys. Rev. D **82**, 103525 (2010).

[169] F. Bezrukov, A. Magnin, M. Shaposhnikov, and S. Sibiryakov, Higgs inflation: Consistency and generalisations, J. High Energy Phys. 01 (2011) 016.

[170] K. Kamada, T. Kobayashi, M. Yamaguchi, and J. Yokoyama, Higgs G-inflation, Phys. Rev. D **83**, 083515 (2011).

[171] K. Kamada, T. Kobayashi, T. Takahashi, M. Yamaguchi, and J. Yokoyama, Generalized Higgs inflation, Phys. Rev. D **86**, 023504 (2012).

[172] F. Bezrukov, The Higgs field as an inflaton, Classical Quantum Gravity **30**, 214001 (2013).
[173] K. Allison, Higgs xi-inflation for the 125–126 GeV Higgs: A two-loop analysis, J. High Energy Phys. 02 (2014) 040.
[174] F. Bezrukov and M. Shaposhnikov, Higgs inflation at the critical point, Phys. Lett. B **734**, 249 (2014).
[175] Y. Hamada, H. Kawai, K. y. Oda, and S. C. Park, Higgs Inflation is Still Alive after the Results from BICEP2, Phys. Rev. Lett. **112**, 241301 (2014).
[176] Y. Hamada, H. Kawai, K. y. Oda, and S. C. Park, Higgs inflation from Standard Model criticality, Phys. Rev. D **91**, 053008 (2015).
[177] A. Salvio and A. Mazumdar, Classical and quantum initial conditions for Higgs inflation, Phys. Lett. B **750**, 194 (2015).
[178] I. D. Saltas, Higgs inflation and quantum gravity: An exact renormalisation group approach, J. Cosmol. Astropart. Phys. 02 (2016) 048.
[179] X. Calmet and I. Kuntz, Higgs Starobinsky inflation, Eur. Phys. J. C **76**, 289 (2016).
[180] R. Jinno, K. Kaneta, and K. y. Oda, Hill-climbing Higgs inflation, Phys. Rev. D **97**, 023523 (2018).
[181] F. Bezrukov, M. Pauly, and J. Rubio, On the robustness of the primordial power spectrum in renormalized Higgs inflation, J. Cosmol. Astropart. Phys. 02 (2018) 040.
[182] M. He, A. A. Starobinsky, and J. Yokoyama, Inflation in the mixed Higgs-R^2 model, J. Cosmol. Astropart. Phys. 05 (2018) 064.
[183] A. Gundhi and C. F. Steinwachs, Scalaron-Higgs inflation, Nucl. Phys. **B954**, 114989 (2020).
[184] J. Rubio, Higgs inflation, Front. Astron. Space Sci. **5**, 50 (2019).
[185] A. Karam, T. Pappas, and K. Tamvakis, Nonminimal Coleman–Weinberg inflation with an R^2 term, J. Cosmol. Astropart. Phys. 02 (2019) 006.
[186] C. F. Steinwachs, Higgs field in cosmology, Fundam. Theor. Phys. **199**, 253 (2020).
[187] D. Y. Cheong, S. M. Lee, and S. C. Park, Progress in Higgs inflation, J. Korean Phys. Soc. **78**, 897 (2021).
[188] R. Durrer, O. Sobol, and S. Vilchinskii, Magnetogenesis in Higgs-Starobinsky inflation, arXiv:2207.05030.
[189] A. Kogut, D. J. Fixsen, D. T. Chuss, J. Dotson, E. Dwek, M. Halpern, G. F. Hinshaw, S. M. Meyer, S. H. Moseley, M. D. Seiffert *et al.*, The primordial inflation explorer (PIXIE): A nulling polarimeter for cosmic microwave background observations, J. Cosmol. Astropart. Phys. 07 (2011) 025.
[190] T. Matsumura, Y. Akiba, K. Arnold, J. Borrill, R. Chendra, Y. Chinone, A. Cukierman, T. Haan, M. Dobbs, A. Dominjon *et al.*, LiteBIRD: Mission overview and focal plane layout, J. Low Temp. Phys. **184**, 824 (2016).